University of Arkansas, Fayetteville

ScholarWorks@UARK

Graduate Theses and Dissertations

5-2018

Computational Fluid Dynamics Model for Air Velocity Through a Poultry Transport Trailer in a Holding Shed

Christian Heymsfield
University of Arkansas, Fayetteville

Follow this and additional works at: https://scholarworks.uark.edu/etd

 Part of the Biological Engineering Commons, and the Biomedical Devices and Instrumentation Commons

Citation

Heymsfield, C. (2018). Computational Fluid Dynamics Model for Air Velocity Through a Poultry Transport Trailer in a Holding Shed. *Graduate Theses and Dissertations* Retrieved from https://scholarworks.uark.edu/etd/2810

This Thesis is brought to you for free and open access by ScholarWorks@UARK. It has been accepted for inclusion in Graduate Theses and Dissertations by an authorized administrator of ScholarWorks@UARK. For more information, please contact scholar@uark.edu, uarepos@uark.edu.

Computational Fluid Dynamics Model for Air Velocity Through a Poultry Transport Trailer in a Holding Shed

A thesis submitted in partial fulfillment
of the requirements for the degree of
Master of Science in Biological Engineering

by

Christian Heymsfield
University of Arkansas
Bachelor of Science in Biological Engineering, 2016

May 2018
University of Arkansas

This thesis is approved for recommendation to the Graduate Council.

_____
Yi Liang, PhD
Thesis Director

_____
Thomas A. Costello, PhD
Committee Member

_____
R. Panneer Selvam, PhD
Committee Member

Abstract

Broiler production in Arkansas was valued at over $3.6 billion in 2013 (University of Arkansas Division of Agriculture Cooperative Extension Service). Consequently, improvement in any phase of the production process can have significant economic impact and animal welfare implications. One area of concern for the poultry industry is thermal stress experienced by the birds after arrival at the processing plant and before they are taken in to be processed, during which time they are left to wait in holding sheds. Various cooling strategies exist to mitigate heat stress in holding sheds, but in most cases it is unlikely that they are optimal. A computational fluid dynamics (CFD) model was developed using the commercial package ANSYS Fluent to simulate airflow through a poultry trailer in a typical holding shed configuration. The CFD model was compared to experimental data gathered from a poultry processing plant in Northwest Arkansas. The CFD model was able to replicate general trends and relative magnitude of air velocity through the trailer. In addition, three different design alternatives were created to evaluate the usefulness of the model as a tool to improve holding shed cooling strategies. This research showed that CFD could be a potential method to simulate conditions on poultry trailers in holding sheds and test various holding shed cooling strategies. However, it was concluded that a more robust system of validation was necessary to prove the accuracy of CFD for this purpose for most applications.

Acknowledgements

I would like to thank Dr. Yi Liang for her help and allowing me to work on this aspect of her research project. Thanks also to my advisors Dr. Costello and Dr. Selvam for their guidance. Thank you to Dr. Gbenga Olatunde for his time and introducing me to Ansys Fluent.

Contents

1. Introduction

During the transportation of poultry, birds can be subjected to extreme heat or cold. These conditions are concerning, because temperature extremes on poultry are a major cause of physiological stress and are the foremost cause of dead birds on arrival (DOAs) (Hoxey et al., 1996; Kettlewell et al. 2001). The national annual averages for DOA percentages from 2000 to 2005 were between 0.35 and 0.37% (Ritz et al., 2005). Assuming an annual US production of 8.5 billion broiler chickens, this accounts for a loss of about 30 million birds. Such losses have large economic ramifications in addition to being an animal welfare issue.

Heat stress in particular has been recognized as a major cause of bird mortality. The range of conditions in which the birds are able to regulate internal body temperature is the thermoneutral zone. The thermoneutral zone for broilers in transit has been found to be 8 to 18 °C (46 to 64 °F) for well-feathered broilers packed densely together, well below typical production and transport conditions (Webster et al., 1993). Consequently, during the summer months, DOA percentages can increase to over 1.0% (Hoxey et al., 1996). Even if birds survive, shrinkage can occur and quality of meat can still be affected by increased toughness (Schwartzkopf-Genswein et al., 2012).

Commercial trailers for carrying chickens from farms to processing plant are composed of groups of modules and are open to the atmosphere during summer months. Transport of poultry to the processing plant utilizes natural ventilation. When birds arrive at the processing plant, trailers are parked in holding sheds, and birds are left to wait for a period of time. Data taken from previous studies in northwest Arkansas has shown this waiting period to range from 90 to 130 minutes (Liang, 2015). Holding sheds utilize ambient air and fan banks in a variety of arrangements for cooling. Fans placed along the sides of trailer modules force air

through the modules, providing a convective cooling effect on the birds. Tunnel ventilation systems are commonly used in poultry houses for this reason. A common goal for tunnel ventilation systems in poultry houses is to generate air velocity of 3.0 m/s (Dozier et al., 2005). Research has shown that 1 m/s airflow over broiler chickens resulted in similar growth rates over 7 weeks to birds raised in still air that is 1°C cooler, while 2 m/s airflow will had the same effect as air that is 3.7 °C cooler (Huffman, 2000). The environment of a poultry house and that of a poultry trailer are not identical however, and packing densities are higher on a trailer. For ventilation of a poultry trailer, Kettlewell et al. (2000) proposed a ventilation rate of 3 m^3/s, equivalent to 2.16 $m^3/hr/kg$ live-weight and corresponding to air velocities of 1 m/s.

Currently, the operation of fans and cooling protocol in poultry holding sheds is not supported by engineering research, and practices vary from plant to plant. For example, at one commercial plant in Springdale, Arkansas, cooling fans are turned on when ambient temperature exceeds 70° F (21.1°C); however, it is unknown whether this practice is optimal. The effectiveness of different fans and fan configurations under varying environmental conditions is not well understood. A study by Ritz et al. (2005) cited the need for future investigation into the number and configuration of holding shed fans, the benefit of evaporative cooling capabilities, and attention to trailer placement within holding sheds.

A field based study testing various cooling scenarios would be costly and time consuming. Testing alternative number and position of fans and placement of poultry trailers may interfere with processing plant operations. Computational fluid dynamics (CFD) could potentially be a cost effective and more convenient way to model conditions within a poultry trailer positioned in a holding shed. CFD is a numerical modeling technique to solve and

analyze problems involving fluid flow. The use of CFD has become more popular in recent years due to increased computing power and ease of use. In this study, a CFD model was created to simulate airflow within a poultry trailer positioned within a typical holding shed. ANSYS Fluent 17.0 software was used for all CFD simulations. ANSYS software is used for a variety of engineering applications, including aerodynamics, heat transfer, and structural studies. Fluent is a program developed by ANSYS for solving problems involving fluid flow, and has been applied in numerous studies pertinent to this research (Bustamante et al., 2013; Gilkeson et al., 2016; Norton et al., 2013).

For this study, adequate knowledge of the holding shed domain and accurate implementation of flow physics into Fluent was necessary. The following sections give a brief introduction to CFD software and its applications in similar studies and then outline the objectives of this research.

1.1 Literature Review

The Navier-Stokes equations are a set of partial differential equations that describe fluid motion. The Navier-Stokes equations account for conservation of mass (1), conservation of momentum (2), and conservation of energy (3). For an incompressible fluid with isothermal properties these are:

$$\frac{\partial \rho}{\partial t} + \frac{\partial}{x_i}(pu_i) = 0 \quad (1)$$

$$\frac{\partial}{\partial t}(\rho u_i) + \frac{\partial}{\partial x_j}\left(\rho u_i u_j\right) = -\frac{\partial p}{\partial x_i} + \frac{\partial \tau_{ij}}{\partial x_j} + \rho g_i + F_i \quad (2)$$

$$\frac{\partial}{\partial t}(\rho c T) + \frac{\partial}{\partial x_j}\left(\rho u_j c T\right) - \frac{\partial}{\partial x_j}\left(\frac{K \partial T}{\partial x_j}\right) = S_T \quad (3)$$

where ρ is fluid density (kg/m^3); t is time (s); x, x_i, x_j are length components (m); u_i, u_j are velocity component (m/s); p is pressure (pa); τ_{ij} is the stress tensor (pa); g_i is gravitational acceleration (m/s^2); F_i is the external body forces in the i direction (N/m^3); c is the specific heat (W/kg*K); T is the temperature (K); K is thermal conductivity (W/m*K); S_T is the thermal source term (W/m^3) (Bustamante et al., 2013).

Discrete solutions for the Navier-Stokes equations are difficult to obtain. In order to simulate fluid flow, CFD follows a series of steps (Norton et al., 2007):

- Creation of a model geometry
- Discretization of model geometry into a finite number of elements (meshing)
- Specification of cell zone conditions and boundary conditions at surface/zone interfaces
- Transformation of partial differential equations for conservation of mass, momentum, and energy within each element to a system of discrete, algebraic equations
- Iterative calculations of the conservation equations until solution convergence
- Analysis of results and validation

Use of CFD in agricultural engineering has become more prevalent in recent years due to advancements in computer technology. Simulations are now faster and more accurate than before, making CFD a valuable tool in a wide range of applications. The advantages of CFD are numerous. Chiefly, CFD enables quick testing of multiple design alternatives, making it a powerful, cost effective and efficient decision-making tool. In addition, researchers can examine a much greater number of points within a problem domain when compared to field measurements (Blanes-Vidal et al., 2008). Furthermore, many CFD programs provide visual

representation of results, such as contours of temperature and pressure and vectors for air velocity.

Due to the importance that ventilation rate and air temperature serve in the thermal comfort of farm animals within their environments, CFD and its capabilities are very attractive. Early applications of CFD modeled the indoor environment of greenhouses. Building on these studies, many publications have used CFD in studies of indoor conditions of swine, poultry, and livestock houses and carriers. In addition, CFD has been used to model polluting emissions from livestock houses. Several of these studies are summarized below.

Dalley et al. (1996) attempted to use numerical modeling to characterize the thermal environment that chickens are exposed to during commercial transport. More specifically, temperature, humidity, and ventilation rate within the transport trailer were calculated. Data from a series of full-scale wind tunnel experiments was used to input boundary conditions in a CFD model. A commercial CFD model was not used; rather, a numerical model based on the conservation of mass and energy was developed. While not as powerful and full featured as CFD models that exist today, the computer model did predict temperature and relative humidity in the trailer over time and space, and showed sensitivity to external environmental conditions and wind direction. The study concluded that computer modeling could be used as a tool to estimate the internal environments of different trailer journeys and configurations (Dalley et al., 1996)

Early versions of commercial CFD software were applied to greenhouse environments. Kacira et al. (1998) used the commercial CFD program Fluent V4 to predict ventilation for different configurations of inlets and outlets in a greenhouse. This early study showed the importance of computer power in CFD studies, as researchers were limited in the size of the

computational domain and calculation times were on the scale of 8 to 24 hours per simulation. Nonetheless, the researchers were able to identify a specific inlet configuration for ideal ventilation rates based on results of the model.

Similar to research on greenhouses, later studies attempted to predict ventilation rates within livestock houses. A research paper by Blanes-Vidal et al. (2008) applied CFD to quantify ventilation rates within a poultry house to identify possible conditions dangerous to the thermal comfort of birds. The CFD code Fluent 6.0 was used. Boundary conditions for inlets and outlets were determined from on-site measurements. Four different boundary condition scenarios were tested. Results from the simulations were validated using air velocity and temperature measurements within an actual poultry house. According to the authors, simulated air results were "a reasonable estimation of velocities in a commercial poultry building" (Blanes-Vidal et al., 2008). CFD simulations over estimated mean air velocities at bird height by 0.18 m/s (0.54 m/s for the simulation compared to 0.36 m/s from measurements) (Blanes-Vidal et al., 2008). The authors concluded that CFD can provide "useful information about the actual airflow in commercial poultry buildings" (Blanes-Vidal et al., 2008). This study did not take into account the presence of chickens within the model and their effect on airflow or heat production.

A similar study by Bustamante et al. (2013) applied the CFD code Fluent to mechanically ventilated poultry houses. Different set ups for number of fans and inlet openings were tested. Results from CFD simulations were validated with a multi-sensor system. CFD results showed close agreement with experimental data (mean of air velocity values was 0.60 ± 0.56 m/s for CFD techniques and 0.64 m/s for direct measurements).

Many CFD programs have the ability to model species transport. Due to this capability, several studies have used CFD to model gaseous emissions from agricultural houses in addition to results for air ventilation and temperature and humidity conditions. Pawar et al. (2007) used a 2D model in the CFD code Fluent to model the spread of virus particles from a poultry house. Two ventilation schemes were tested, and one was found to better limit the spread of contaminants downwind. However, CFD simulations in this study were not validated with experimental data. A study by Rong et al. (2015) used CFD to model ammonia emissions from a swine house. CFD also has been used to simulate gas mixing within swine houses (Stikeleather et al., 2012).

More pertinent to this study, examples of the application of CFD to model airflow through poultry and livestock trailers do exist, though in fewer quantities than those concerned with poultry or livestock houses. Gilkeson et al. (2016) used the commercial CFD package ANSYS Fluent to simulate passive ventilation through a livestock trailer pulled by a generic towing vehicle. Notable in this study was the coupling of internal and external flow domains; that is, air flowing around the vehicle and trailer and through the trailer. Results from the computer simulation showed reasonable agreement to wind tunnel measurements for a $1/7^{th}$ scale model from a previous study (Gilkeson et al., 2009). Researchers were also able to suggest improvements to common trailer design to facilitate better airflow through the lower portion of the trailer.

A study by Hui (2013) sought to develop and validate a CFD model to quantify ventilation and thermal conditions on poultry trailers subjected to winter conditions in Canada. The study consisted of multiple parts, including the design of an actively heated and ventilated experimental vehicle; field testing of this experimental vehicle; development, calibration, and

validation of CFD models to simulate environmental conditions within experimental trailer; and usage of the CFD model to test different design alternatives. Notable in this study was the use of a porous media solution to approximate the influence of chickens on airflow through poultry modules. Viscous and inertial resistance coefficients were chosen based on the dimensions of chicken forms and volume relative to the empty space within each module (Hui, 2013).

Concerning porous media, the benefits of using this technique are significantly reduced mesh size and improved calculation speed and accuracy. Wu et al. (2012) used a porous model to represent the animal occupied zone (AOZ) in a study for determining air exchange rates within a naturally ventilated dairy cattle building. Resistance coefficients for the porous media were found using a sub-model. The sub-model consisted of four model cows arranged within a part of the building. The pressure drop across the domain for numerous air velocities was then found and used to quantify resistance coefficients for the porous media model.

Rong et al. (2015) used porous media to model the slatted floors of a pig house in a study on ammonia emissions from underground manure storage. The porous media model was not able to predict air speed accurately above the floor; however, results for ammonia emissions from the porous media model were comparable to results from a slatted floor CFD model.

In contrast to the porous media approach, some studies have used simple geometric shapes to simulate the impact of animal forms on airflow, and also included models for animal heat and moisture production. Pawar et al. (2007) represented hens as blocks specified as walls in the CFD model Fluent. The walls were given a boundary condition of constant heat flux to model heat generated by the hens. The heat flux calculated was equal to the basal metabolic rate of the hens. However, in actual scenarios, heat loss from animals is dependent on the air

temperature, air velocity, coat thickness, and long wave and solar radiation (Turnpenny et al., 2000).

A study by Norton et al. (2013) showed the effectiveness of explicitly modeling cattle to predict the temperature and relative humidity in mechanically and naturally ventilated livestock transportation trailers. Cattle were modeled as half ellipsoids with varying heat and moisture loss based on environmental temperature (Norton et al., 2013). STAR-CCM+ software was used. A boundary condition of constant outward velocity represented the fans in the mechanically ventilated trailer, while the naturally ventilated condition used a pressure outlet and relied on internal buoyancy generation for air flow. Results showed that mechanically ventilated trailers had less homogenous conditions, a fact that could be concerning in winter months, when low ventilation rates could cause poor air quality in some parts of the trailer (Norton et al., 2013).

Research in CFD modeling showed that proper selection of spatial dimensionality, namely the choice of two spatial dimensions or three, was imperative to each study. The selection of modeling in two dimensions or three dimensions should consider the objectives of the model and flow physics of the problem. The advantage of a 2D model is a highly reduced mesh size with much faster and greater ease of computation. The size of a 3D model requires the user to have access to high performance computational resources in order to perform simulations; a 2D model can be simulated with average computer resources. However, 2D models are inherently limited because they consider only a cross section of 3D model geometry, and geometrical symmetry as well as flow symmetry is assumed around the plane being modeled. Studies utilizing a 3D model have already been mentioned (Bustamante et al., 2013; Norton et al., 2013; Gilkeson et al., 2016). Previous studies using a 2D model include the

modeling of heat and mass transfer within a poultry house (Rojano et al., 2015) and the spread of gaseous particles from a poultry house (Pawar et al., 2007). Rojano et al. (2015) found that the CFD model produced acceptable results for two dissimilar cases. The research by Pawar et al. (2007) led the authors to make a recommendation for ventilation systems in poultry houses. Both studies coupled indoor and outdoor flow of poultry houses.

1.2 Example Holding Shed Location and Details

As previously stated, holding shed practices can vary widely from location to location. An example is described here in order to give the reader an idea of a possible holding shed configuration. At one processing plant in Springdale, AR, poultry transport trailers are brought into holding sheds covered by a sloping metal roof but open at the sides. On the poultry trailers are rows of modules in which chickens are contained. Typically, 10 or 11 rows are lined up going the length of the trailer, and one module is stacked on top of another, for a total of 20 or 22 modules. The module structure is made of a galvanized steel frame with five fiberglass floors, dividing each module into five tiers. Chickens are loaded into the tiers of the module through a set of spring-loaded doors. The front, back, and opposite side consist of a metal latticework that does little to obstruct airflow.

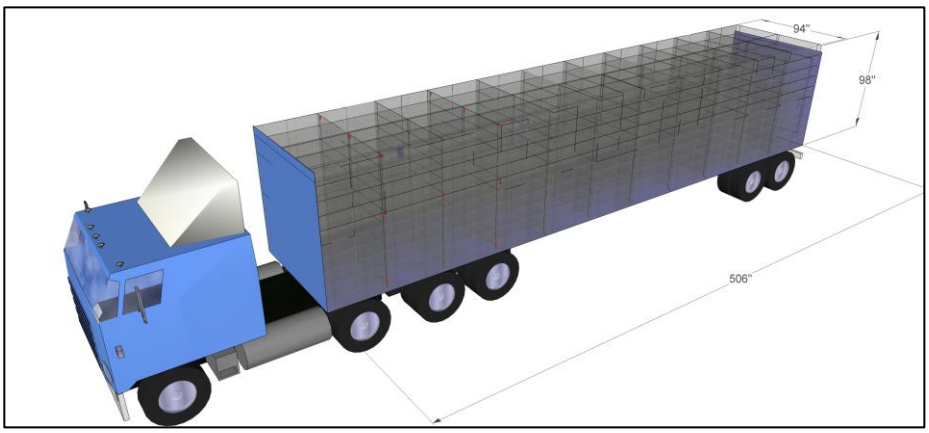

Figure 1.1: Modules arranged on trailer

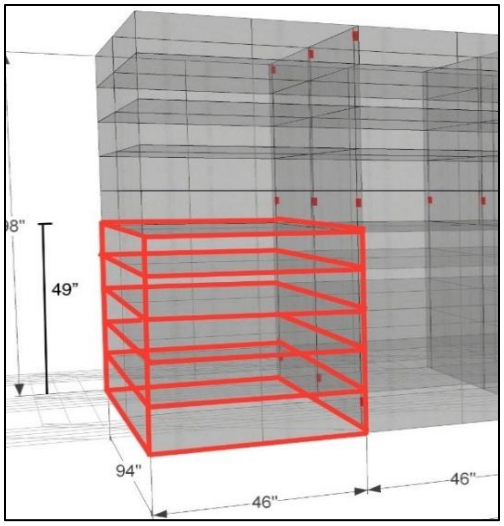

Figure 1.2: Module dimensions. Four modules are shown. Red outlines show one module divided into five floors.

Within the holding sheds at the study plant, the trucks park two wide next to a series of fan banks. Fans measured at the site were 1.22 m (48 in.) in diameter. At the site, six fans are arranged in a row, with fan rows placed on opposite sides of the shed blowing air onto the adjacent trailers (figure 1.3). The fans at the site were positioned 2.24 m (88 in.) from the ground to the bottom of the fan and 1.27 m (50 in.) horizontally from the trailer, at a slight downward angle.

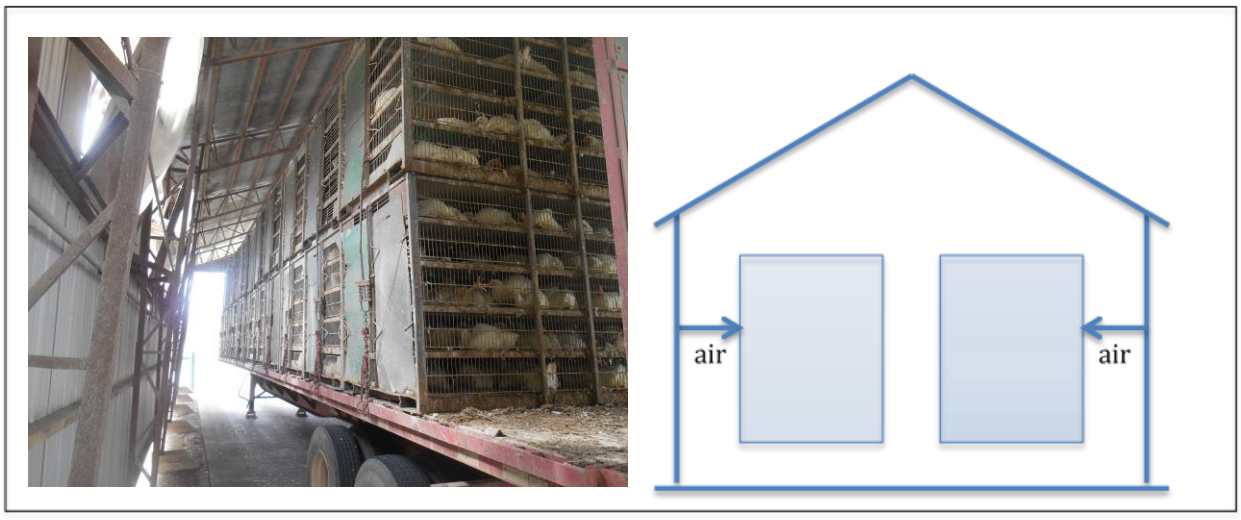

Figure 1.3: Loaded poultry trailer parked in shed at the test site

Figure 1.4: Filled trailer parked within holding shed at the test site

1.3 Objectives

The objectives for this study were as follows:

- Development of a CFD model with the ability to predict air velocity in the internal environment of a fully loaded poultry trailer in a typical holding shed
- Comparison of CFD simulation results with data collected from a poultry processing plant holding shed
- Testing of alternative cooling strategies for holding sheds using the CFD model
- Assessment of the accuracy and potential of CFD for modeling airflow conditions within a poultry trailer holding shed
- Recommendations for future research

This research was done in conjunction with a larger study undertaken by Dr. Yi Liang of the University of Arkansas Biological and Agricultural Engineering Department. Further objectives of the larger study include characterizing the thermal microenvironment on broiler trailers during both transport and holding shed times during three seasons of the year, and the development of an electronic chicken to quantify heat exchange of broiler chickens within poultry trailers (Luthra et al., 2018).

2. CFD Model Set Up

2.1 Geometry and Meshing

Despite the benefits of 2D modeling, a 3D model was chosen for this study after consideration of model objectives and data taken from the test site. Data collected from a typical poultry trailer holding shed showed that air velocity decayed in the same vertical cross section with increasing distance from the fan. This implies that there is airflow with velocity components perpendicular to this cross section, making a 2D model less valid to this study.

Geometry editing was done using ANSYS Design Modeler Software. A simplified geometry was created with placement of features similar to the holding shed at the test site; only a subsection of the holding shed that included three stacks of two modules each and two exhaust fans was included. It was assumed that conditions within the four modules of interest were not affected by airflow from fans nor other modules not included in this subsection. In addition, a symmetry condition was specified at one end of the domain, splitting one of the fans in half. Previous CFD studies have utilized this symmetry boundary condition to reduce mesh size (Norton et al., 2013). The stacks of modules were separated by a distance of 0.15 m (6 in.). The modules were positioned 1.22 m (48 in.) from the ground. Geometry of the trailer in which the modules are usually placed was not included. The geometry of each module was simplified; wire meshing on the face of the trailers and some metal supports were not included. These parts were considered to have negligible effect on airflow in and around the modules and would add greatly to mesh size and computational time. Fans were modeled as cylinders of radius 0.61 m (24 in.) and thickness 0.10 m (4 in.). For default simulation, these fans were positioned 2.26 m (89 in.) vertically from the ground and 1.22 m (48 in.) horizontally from the face of the trailer, with the axis of one fan positioned in the horizontal center of one set of modules and the axis of the other fan positioned off-center to resemble placement at the testing site. The fans were also given a

downward tilt of 10°. A large enclosure surrounded modules and fans to minimize disturbance of airflow in and around the fan and modules. The domain was divided into sections to allow for a finer mesh in the area of modules and fan. Chicken forms were not explicitly modeled; rather, the animal occupied zone was considered porous media. Set up of the animal occupied zone is described in section 2.3. The total size of the domain was 8.84m x 8.79m x 21.49m. Meshing was completed using the ANSYS meshing utility. In areas subject to more airflow, fineness of the mesh was increased. Total size of the final mesh was 4,807,192 elements, consisting of both hexahedral and tetrahedral elements, and 1,007,722 nodes.

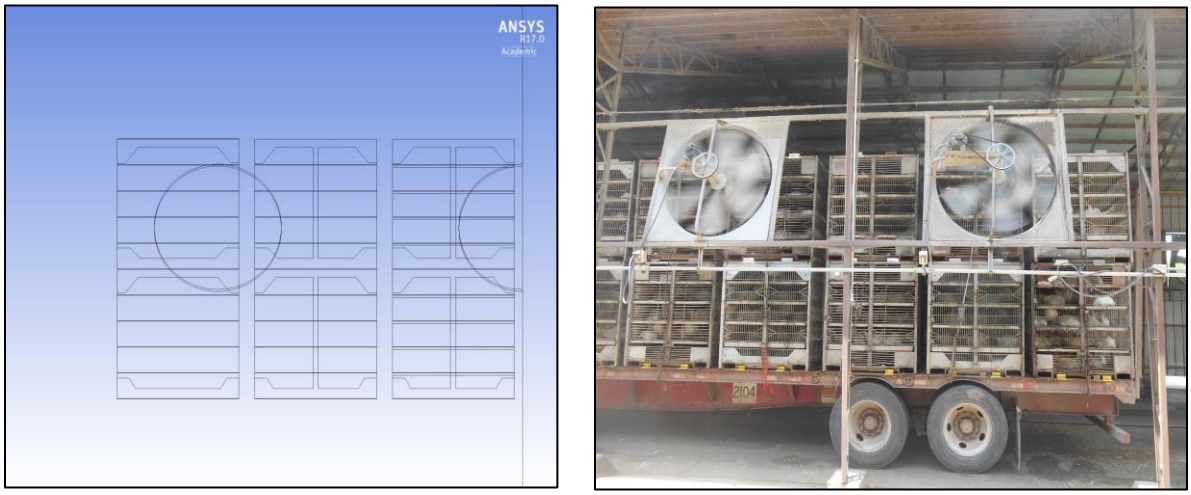

Figure 2.1: Comparison of model geometry and trailer at the test site. Vertical plane to the right in model geometry has symmetry boundary condition

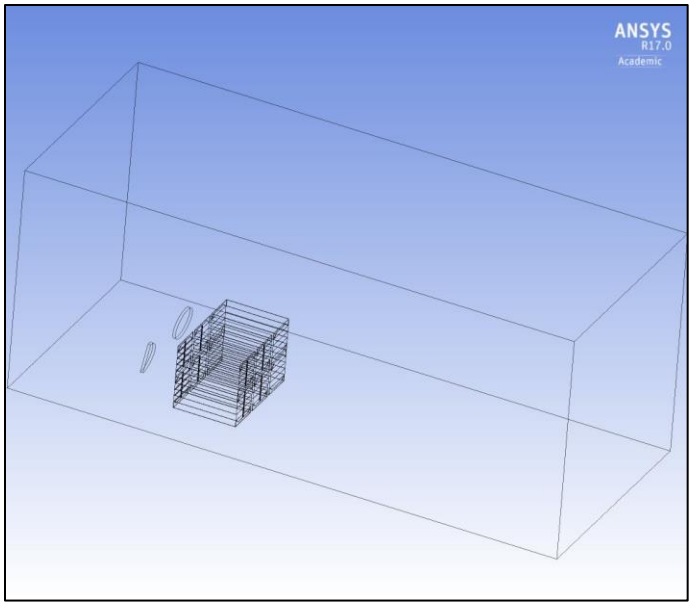

Figure 2.2: Isometric view of entire model domain

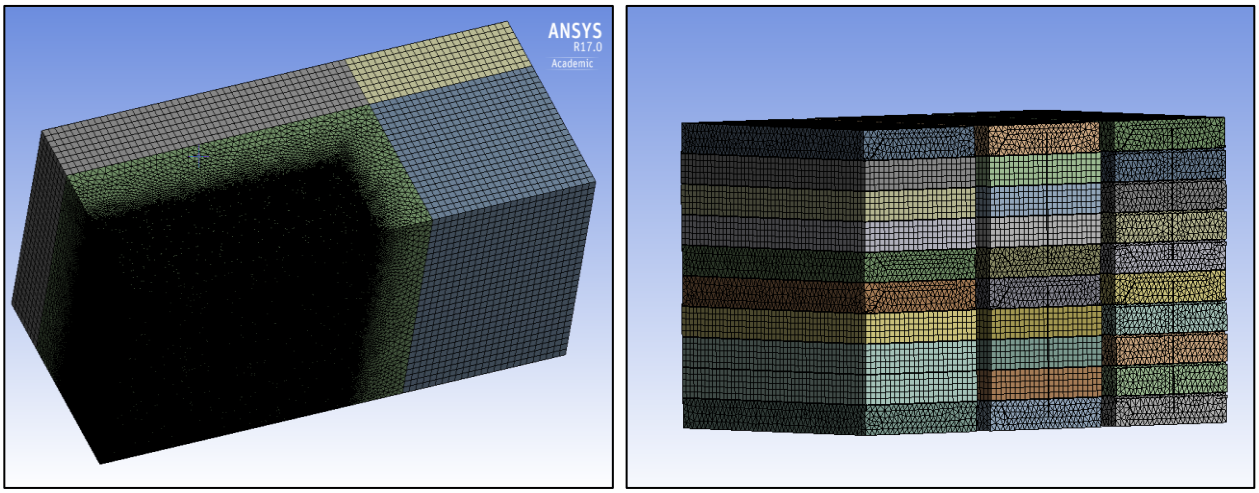

Figure 2.3: Surface mesh of entire domain and surface mesh of modules. Mesh was created finer near modules.

2.2 Boundary Conditions and Computational Models

Pressure outlet with 0 pa gauge pressure was specified at the faces of the domain behind and to the left side of modules from the perspective of the fan outlets. Pressure inlet with 0 pa gauge was specified at the face of the domain upwind of flow from the fans. The fans were modeled using the 3D fan zone within ANSYS Fluent. The 3D fan zone is a fluid cell zone that simulates the effect of an axial fan, accounting for swirl and radial velocities (ANSYS

Fluent). The input conditions for a 3D fan zone within Fluent include a pressure jump and angular velocity. A typical fan used by poultry processors with diameter similar to those at the experimental site has an airflow rate of 21,700 ft^3/min, or approximately 10.24 m^3/s (acmefan.com). This value was converted to a pressure jump, ΔP, by conservation of energy, where A_{fan} is the surface area of the face of the fan:

$$\Delta P = \frac{1}{2}\rho_{air} v^2$$

$$v = 10.24\ \frac{m^3}{s} / A_{fan}$$

$$A_{fan} = \pi * (\frac{1.22m}{2})^2$$

$$v \approx 8.78\ m/s$$

$$\Delta P = \frac{1}{2}\rho_{air} v^2 = \frac{1}{2}\left(1.225\frac{kg}{m^3}\right) * (8.78\frac{m}{s})^2 \approx 47.2\ pa$$

For angular velocity:

$$382\ rpm \approx 40\ rad/s$$

Doors were implemented into the geometry by specifying the corresponding faces of each module using named selections. Chickens were modeled as porous media, with parameters determined from a sub-model. Likewise, the lattice of metal bars on the front and back faces of modules was modeled using a porous jump condition, with parameters also determined from a sub-model. Walls and doors of the modules were specified as walls with no slip boundary condition. Cell zone and boundary zone conditions are summarized below.

Cell Zone and Boundary Conditions:

- Walls, floors, and doors: Wall, no slip
- Domain within modules: Porous media
    - Inertial resistance (1/m) $C_2 = 3.14$
    - Viscous resistance ($1/m^2$), $1/\alpha = 57{,}755$
    - Porosity = 0.80
- Metal bars on front and back faces of modules: Porous jump
    - Face permeability (m^2), $\alpha = 1.12 \times 10^{-6}$
    - Pressure jump coefficient (1/m), $C_2 = 14.1$
    - Porous medium thickness = 0.006 m
- Fan outlets: 3D Fan Zone
    - Constant pressure jump = 47.2 Pa
    - Operating angular velocity = 40 rad/s
- Pressure inlet: 0 Pa gauge
- Pressure outlets: 0 Pa gauge

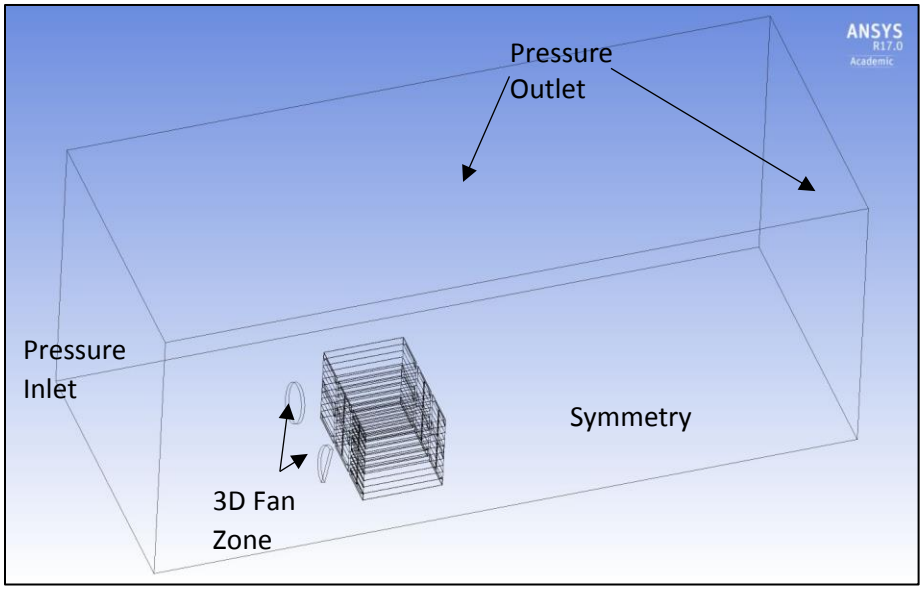

Figure 2.4: Boundary conditions

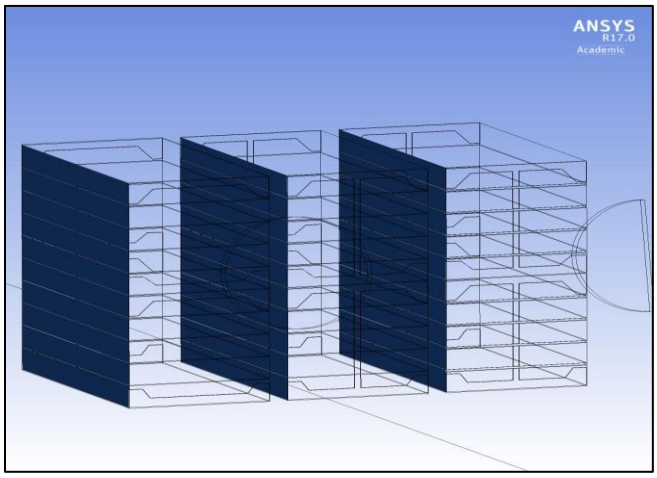

Figure 2.5: Faces highlighted were specified as "doors" with wall boundary condition. Faces directly opposite allowed air to move freely through.

2.3 Modeling the Animal Occupied Zone (AOZ)

The inclusion of explicit chicken forms within the model would lead to significant increases in computational time and effort due to the large number of cells required. Furthermore, simulation using explicit animal forms would impose unrealistic conditions on the model; specifically, local conditions of air velocity and temperature would be dependent on the arbitrary positioning of bird forms within the module. Additionally, it would be difficult to account for movement of birds during simulation of time. A homogenous condition, while not

completely realistic, would give more accurate information regarding general patterns of air velocity and temperature within the modules. For these reasons, an alternative method to account for the resistance to airflow and heat production caused by the presence of poultry was used; the area occupied by the birds, designated the animal occupied zone (AOZ), was approximated as porous media with resistance to airflow similar to that posed by poultry within a cage with a certain loading density.

2.3.1 Porous Media Sub-model

Numerically quantifying the air resistance of poultry was done with the aid of a sub-model within ANSYS Fluent, as seen in Wu et al, (2012). First, it was necessary to consider the loading density and size of birds within the module to calculate parameters for the porous media zone. The loading density of 2.5 kg birds is approximately 220 birds per module. A module having five floors will thus contain approximately 44 birds per floor. In the model, the dimensions of each floor were 1.17 m (46 in.) wide and 2.44 m (96 in.) long. The loading density on a floor area basis then equates to

$$44\ {birds}/{1.17m * 2.44m} = 15.41\ {birds}/{m^2} = 0.065\ {m^2}/{bird}$$

The height of each floor is approximately 0.25 meters. It was assumed that the birds are evenly distributed and that no birds are stacked upon one another. Therefore, the sub-model included one bird occupying a volume of 0.254 meters long by 0.254 meters wide or 0.065 square meters with height 0.25 meters. It was observed that most birds assume a sitting position within the trailer. The skin surface area of a chicken can be approximated by the following equation (Aerts and Berckmans, 2004):

$$A_s = 0.081W^{0.667}$$

Where A_s is skin surface area (m^2) and W is mass (kg). For a 2.5 kg bird, this equates to

$$A_s \approx 0.15m^2$$

A single chicken was modeled having skin surface area approximately 0.15 square meters with the general morphology of a chicken.

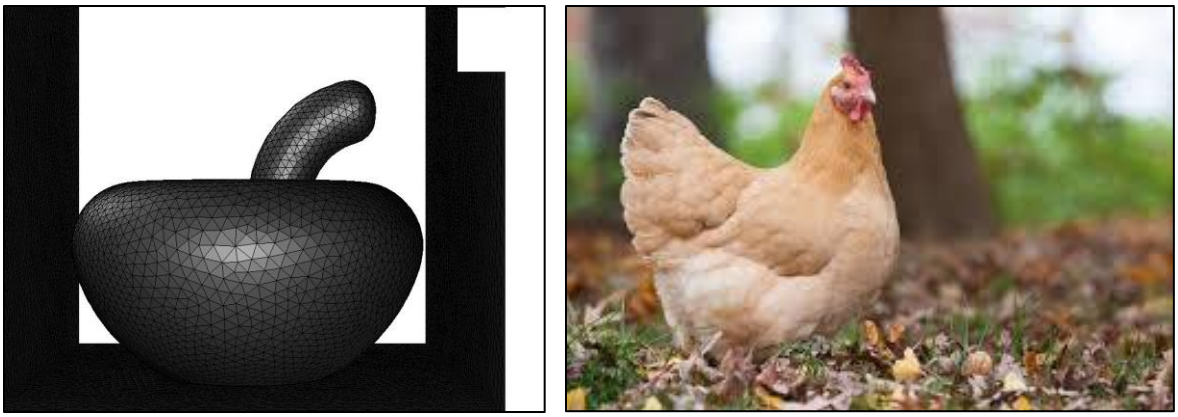

Figure 2.6: View of chicken form created for porous media sub-model, and comparison to an actual chicken

The porous media model within ANSYS Fluent requires values for flow resistance parameters. For simple homogenous porous media

$$S_i = -\frac{\mu}{\alpha} v_i + C_2 \frac{1}{2} \rho |v| v_i$$

where S_i is the source (or sink) term for the *i*th momentum equation, $|v|$ is the magnitude of velocity, μ is the viscosity, α is the permeability, ρ is the density, and C_2 is the inertial resistance factor. Running the sub-model yielded the following pressure drops for the following inlet velocities:

Table 2.1: Calibration data from porous media sub model

Velocity (m/s)	Pressure drop (Pa)
1	0.72
1.5	1.49
2	2.51
2.5	3.72
3	5.17

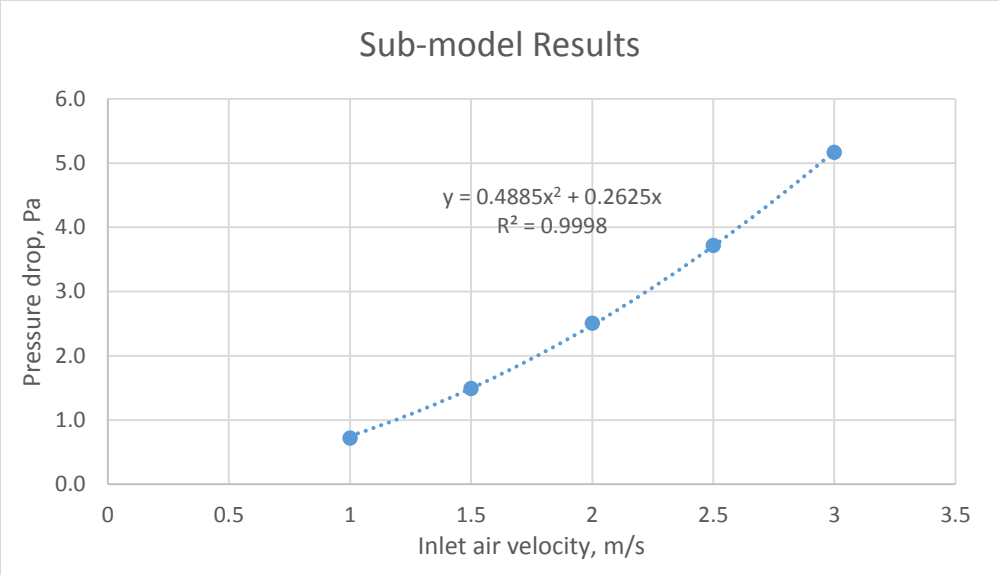

Figure 2.7: Graph of sub model calibration data with trendline

A trendline through these points yields the following equation:

$$\Delta P = 0.4885v^2 + 0.2625v$$

Note that a simplified version of the momentum equation can be expressed as

$$\Delta P = S_i \Delta n$$

where *Δn* is the length of the porous media in the direction of the flow. Comparing the trendline equation to the above equation gives the following identities:

$$0.4885 = C_2 \frac{1}{2} \rho \Delta n$$

$$0.2625 = \frac{\mu}{\alpha} \Delta n$$

With $\rho = 1.225\ {}^{kg}/_{m^3}$, $\Delta n = 0.254\ m$, and $\mu = 1.7894\ x\ 10^5\ Pa \cdot s$ the values for inertial and viscous resistance coefficients are, respectively:

$$C_2 = 3.14$$

$$\frac{1}{\alpha} = 57{,}755$$

In addition, the porosity of the media was considered, with bird volume taken from chicken volume of the sub-model:

$$Total\ bird\ volume = 44\ birds * \frac{0.00317m^3}{1\ bird} = 0.1395m^3$$

$$Porosity = \frac{Void\ volume}{Total\ volume} = \frac{(1.17m * 2.44m * 0.25m) - 0.1395m^3}{1.17m * 2.44m * 0.25m} = 0.80$$

These values were used for porous media zone resistance within the final model.

In a similar method, the effect on airflow of the array of metal bars on the front and back faces of poultry modules was accounted for. This feature is shown in figure 2.8, along with the geometry of the sub model.

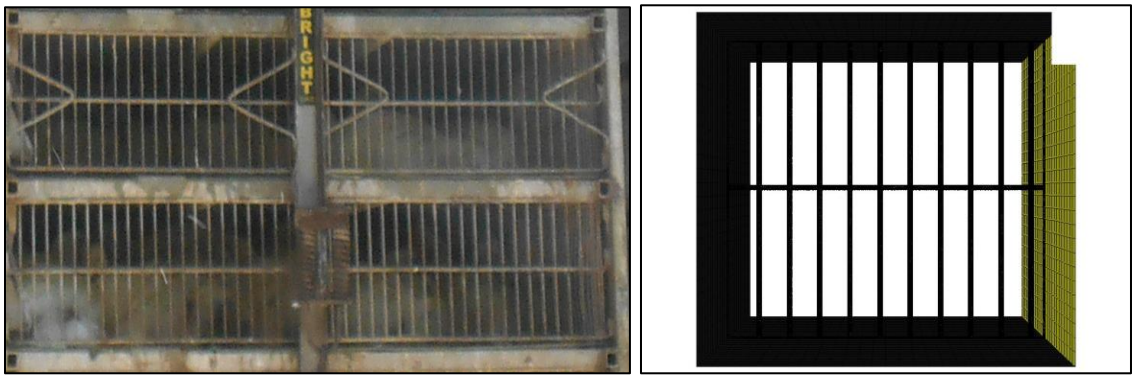

Figure 2.8: Metal bars on face of modules and sub model

Using measured values for pressure drop for five different inlet velocities tested, the following parameters were determined from a calibration curve of the data:

$$C_2 = 14.1$$

$$\alpha = 1.12 \times 10^{-6}$$

2.4 Solution Methods

Pressure based solver was used all simulations. The airflow within the module was assumed turbulent, which is common among ventilating flows (Norton et al, 2010). The standard k-epsilon model was used with standard wall functions as it has been applied numerous times in similar applications (Bustamente et al, 2013; Norton et al, 2010; Pawar et al, 2007). A summary of the solution methods used for simulations is given below.

Solution Methods:

- Pressure-Velocity Coupling: SIMPLE
- Gradient: Least Squares Cell Based
- Pressure: Second Order
- Momentum: Second Order Upwind
- Turbulent Dissipation Rate: Second Order Upwind

Simulations were solved using the University of Arkansas High Performance Computing Center (HPCC). Simulations were run in steady state condition. Typically ANSYS Fluent considers calculations converged when residual values of $1x10^{-3}$ for continuity, x-velocity, y-velocity, and z-velocity, k, and epsilon are reached. However, these criteria are not always a good metric for convergence. Therefore, for all simulations, these convergence criteria for residuals were turned off, and velocity magnitudes at specific points were observed until they reached steady values to determine convergence. The time required for the solution to reach the desired level of convergence was approximately five hours and 56 minutes.

2.5 CFD Model Sensitivity Analysis

A sensitivity analysis was necessary to observe how changes in key model parameters affected simulation results. Uncertainty existed for many input parameters in the model.

However, examining all of the input parameters in a CFD model, including geometry and boundary conditions, physics models, and solution methods, would be time consuming and wasn't feasible for the scope of this study. Input parameters chosen for the sensitivity analysis were selected because it was likely that changes to these parameters would affect solutions in expected ways, and they were also related to key boundary conditions. Base values for these parameters have been discussed in the previous section. They are identified as the "default" values in table 2.2. Six simulations with different values for the chosen parameters were tested: fan pressure jump included three separate conditions, and AOZ viscous resistance included three separate conditions. For each simulation, the value of one input parameter was changed, and all other input parameters were given "default" values. This equated to a total of six separate simulations, not including the default simulation. The input parameters identified for this study, as well as a description of each of the values tested in the sensitivity analysis, is shown in table 2.2:

Table 2.2: Input parameters chosen for sensitivity analysis

Input Parameter	Default	Condition 1	Condition 2	Condition 3
Fan Pressure Jump (Pa)	47.2	41.5	54.5	80.5
AOZ Viscous Resistance	57,755	20,000	40,000	80,000

3. Experimental Procedure

To ascertain typical conditions on a poultry trailer during summer months, a poultry trailer was equipped with sensors to determine air velocity and temperature conditions at various locations within the poultry modules. Sensors used were Kestrel 5000 Series Livestock Environmental Meters (kestrelmeters.com). The Kestrel sensors were fixed in place within poultry modules, and did not have the ability to orient themselves to the predominant direction of airflow. The logging interval was set at 5 seconds. The sensors were placed within four modules; both top and bottom modules located at rows five and six from the driver were equipped with sensors. For row five, six sensors were installed in each module; 3 sensors were installed on each of two floors, with one sensor on the passenger side, one in the center, and one on the driver side, all located along the centerline of the module. The top module for row six was equipped similarly, while the bottom module for row 6 contained only one floor of sensors, or three total. Blue bars in the figure below indicate where the sensors were installed. The location of these sensors is described in figure 3.1

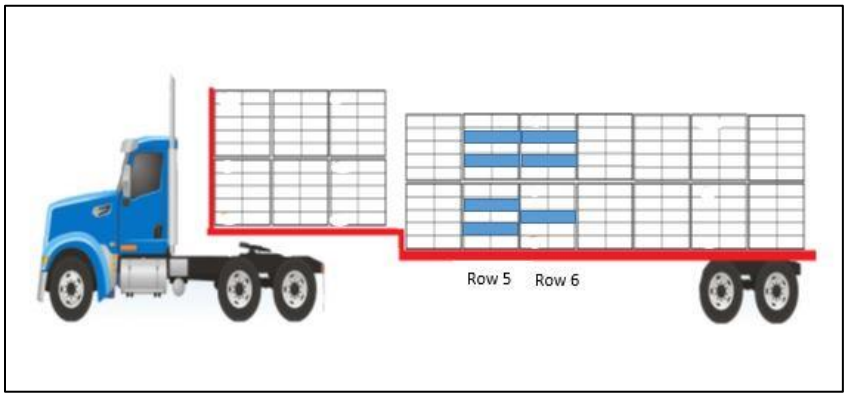

Figure 3.1: Blue bars indicate floors equipped with sensors. For each floor, three sensors were equipped along the centerline: one near the fan side of modules, one near the far side of modules, and one halfway in between the two sides.

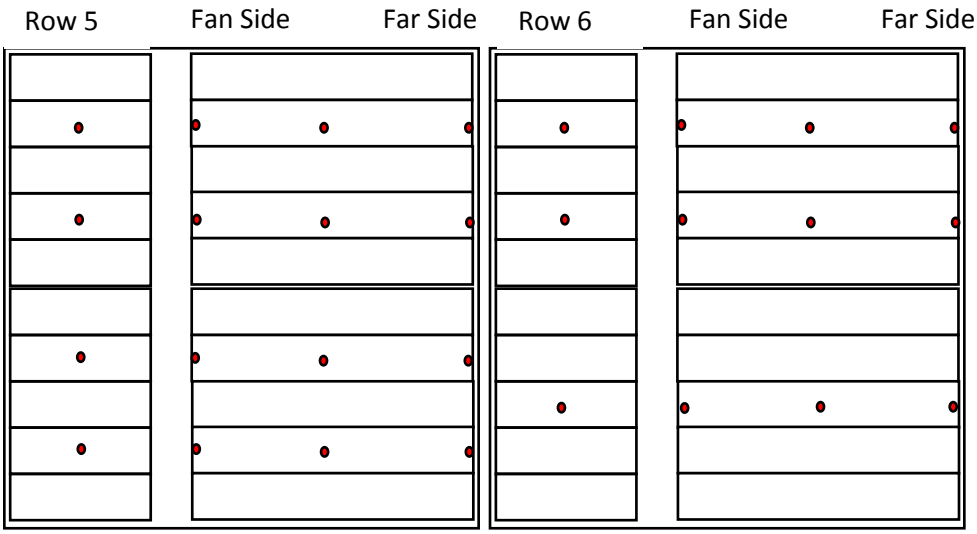

Figure 3.2: Head on and side views of sensor placement within modules

The test was conducted on June 27, 2017. Weather conditions were sunny with mild wind. The loaded trailer was parked in the holding shed from 12:30 pm to 2:25 pm on the day of testing. The trailer was oriented so that the driver side was near to the fan bank.

Figure 3.3: Poultry trailer within holding shed on the day of testing

4. Results and Discussion

4.1 Data from the Test Site

Values recorded in table 4.1 are equally weighted averages of all sensors in each region of the trailer specified. For example, values for "Row 5 Center" are average values for temperature and air velocity of the four sensors located in this region. Table 4.2 considers only air velocity data while all sensors are included. Table 4.1 and table 4.2 data are time averaged for the duration of the holding shed period.

Table 4.1: Averaged temperature and air velocity values within trailer modules; average of three sensors for each region, n=1379 for each sensor

Trailer Region	Temperature, °C	Air Velocity, m/s
Row 5 Fan Side	29.1	1.3
Row 5 Center	29.6	0.8
Row 5 Far Side	28.8	0.7
Row 6 Fan Side	28.5	1.8
Row 6 Center	29.1	1.3
Row 6 Far Side	28.5	1.3
Ambient Outside Trailer	27.8	

Table 4.2: Average air velocity (m/s) values for all sensors within trailer modules, ± one standard deviation, n=1379

Trailer Region	Top	Top Middle	Bottom Middle	Bottom
Row 5 Fan Side	1.2 ± 0.6	1.4 ± 0.7	NA	1.3 ± 0.6
Row 5 Center	0.6 ± 0.4	1.1 ± 0.6	0.6 ± 0.4	1.0 ± 0.5
Row 5 Far Side	0.9 ± 0.4	1.0 ± 0.4	0.6 ± 0.5	0.4 ± 0.5
Row 6 Fan Side	1.6 ± 0.8	2.7 ± 1.1		1 ± 0.6
Row 6 Center	1.2 ± 1.1	1.8 ± 1.0		1 ± 0.5
Row 6 Far Side	0.6 ± 0.6	1.3 ± 0.6		NA

Although temperature within modules was not considered in the CFD model, this parameter is vital to the well-being of poultry; combined with the effects of humidity and air

velocity, it can be used to predict the effects that a certain set of environmental conditions would have on the internal body temperature of a broiler chicken (Tao and Xin, 2003). Furthermore, local temperature values are most likely correlated with local air velocities, due to the convective cooling effect brought about by moving air. Temperatures within the poultry trailer were 0.7-1.8°C above ambient, with the highest temperatures recorded in the center of modules.

Interesting to note is that local air velocity decreased from fan side to far side (moving down the table) with increasing distance from the fan for both rows 5 and 6. In addition, air velocities for row 6 were higher, most likely a cause of row 6 being in a position relative to the fan that would allow it to capture more air than row 5. Finally, recorded air velocities were highest for the top and top middle module floors. The high placement of the fans within the holding shed should explain this phenomenon; more of the air coming from the fans was incident on this area of the modules.

Table 4.2 also shows values for standard deviation for air velocity at each location where data was collected. In comparison to the measured velocity values, standard deviations are relatively high. High standard deviations may indicate the turbulent or unsteady nature of flow. Additionally, point data taken within trailers may be affected by the movement of birds within modules; a sensor may at one moment be blocked by a chicken and unblocked at another time. These results suggest the difficulty of obtaining reliable data from within poultry trailers during study. Furthermore, the nature and relatively small amount of data collected makes it hard to classify conditions on poultry trailers or validate the CFD model to a high degree. Nevertheless, field data from the test site was useful for showing general trends and magnitudes of air velocities within poultry trailers positioned in a holding shed and served as some measure of comparison for the CFD model.

4.2 Simulated Data from CFD Model

As mentioned, data from the test site was applied to compare CFD results to data from an actual poultry trailer holding shed. Points within the CFD model with geometrically similar locations to the sensors placed on the trailer modules during the experimental study were monitored for air velocity. Comparison of experimental and simulated results are presented below.

Table 4.4: Comparison of measured point data and simulated point data for air velocity, row 5

Trailer Region	Measured (m/s)	Simulated (m/s)
Row 5 Fan Side (Top)	1.2	1.1
Row 5 Center (Top)	0.6	0.8
Row 5 Far Side (Top)	0.9	0.6
Row 5 Fan Side (Top-middle)	1.4	1.5
Row 5 Center (Top-middle)	1.1	1.3
Row 5 Far Side (Top-middle)	1.0	0.8
Row 5 Fan Side (Bottom-middle)	Na	1.2
Row 5 Center (Bottom-middle)	0.6	0.7
Row 5 Far Side (Bottom-middle)	0.6	0.7
Row 5 Fan Side (Bottom)	1.3	0.6
Row 5 Center (Bottom)	1.0	0.3
Row 5 Far Side (Bottom)	0.4	0.2

Table 4.5: Comparison of measured point data and simulated point data for air velocity, row 6

Trailer Region	Measured (m/s)	Simulated (m/s)
Row 6 Driver Side (Top)	1.6	1.9
Row 6 Center (Top)	1.2	0.9
Row 6 Far Side (Top)	0.6	0.8
Row 6 Fan Side (Top-middle)	2.7	2.3
Row 6 Center (Top-middle)	1.8	1.2
Row 6 Far Side (Top-middle)	1.3	1.0
Row 6 Fan Side (Bottom)	1	1.4
Row 6 Center (Bottom)	1	0.5
Row 6 Far (Bottom)	NA	0.4

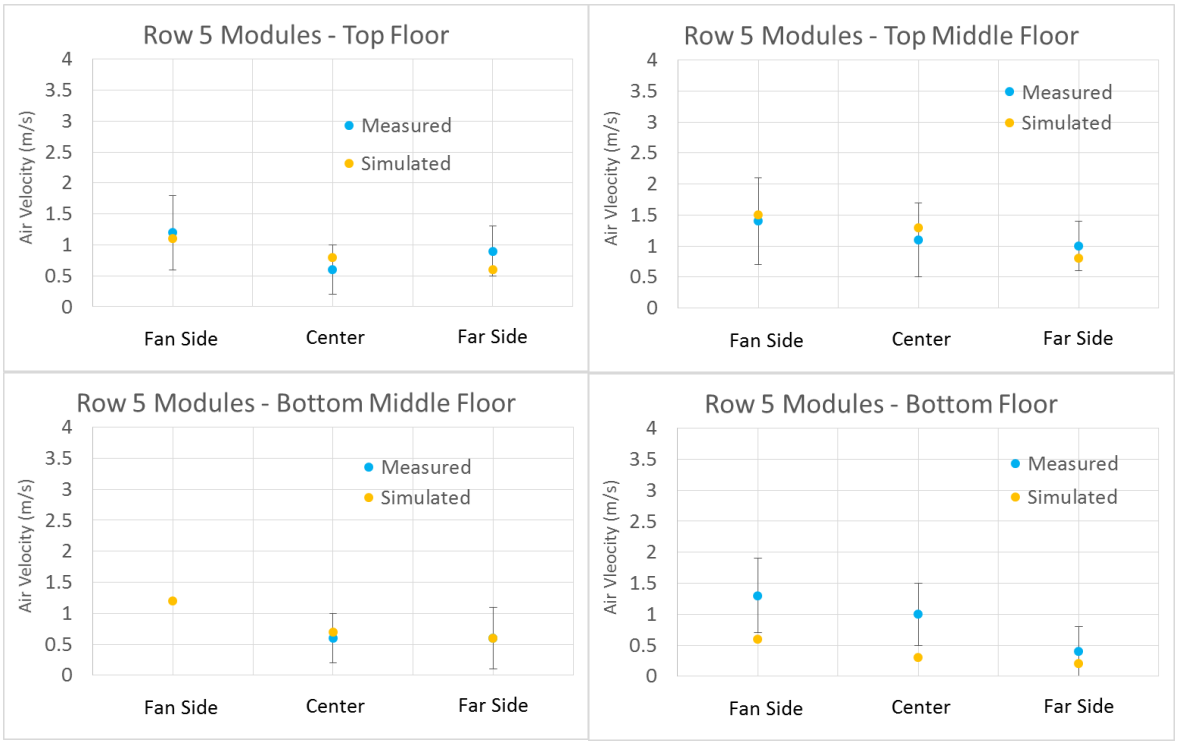

Figure 4.1: Air velocity for row 5 modules, measured and simulated data. Error bars show one standard deviation for measured data, n = 1379

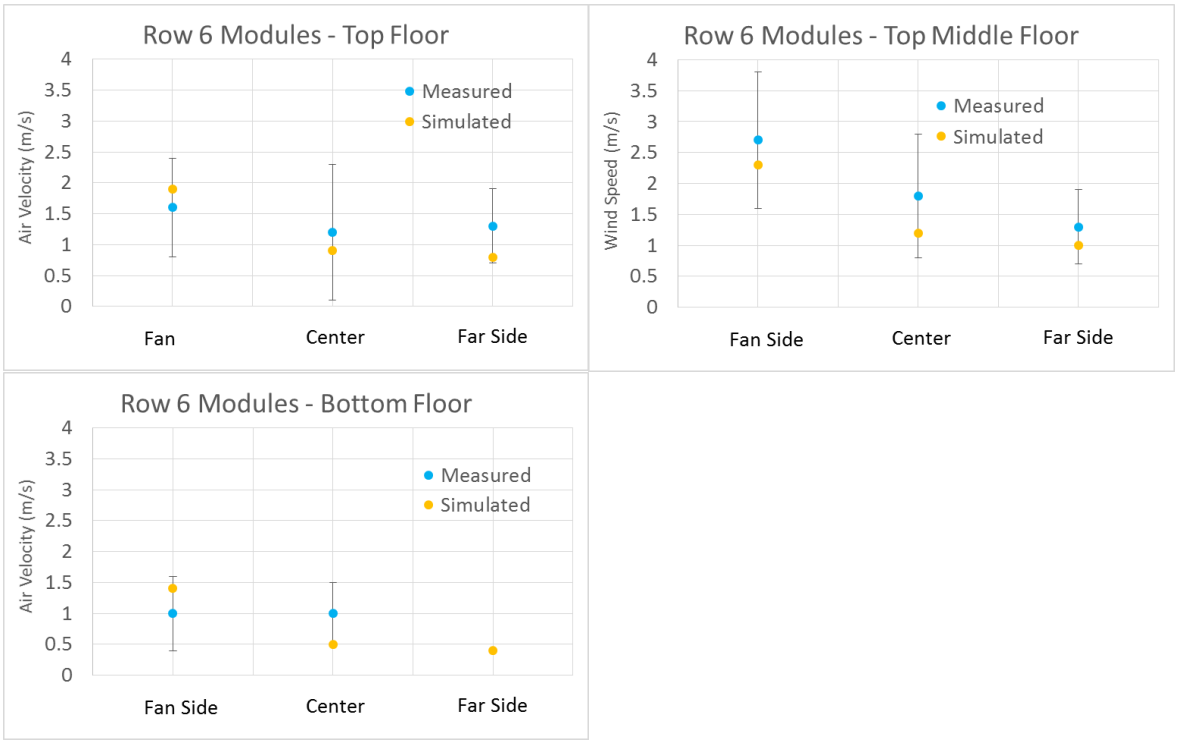

Figure 4.2: Air velocity for row 6 modules, measured and simulated data. Error bars show one standard deviation for measured data, n = 1379

Results from the CFD model had reasonable agreement with measured field data from the test site. Simulated values were all within one standard deviation of experimental values but for a few exceptions. Most noticeable was the underestimation of air velocity through the bottom floor of row 5 modules. This phenomenon was also observed for the center region of the bottom floor of row 6 modules. In addition, for row 6, simulated air velocity at the was underestimated through the top middle floor at all three locations

CFD simulation was able to replicate general observed trends in air velocity through the modules. The trends observed in both experimental and simulated results included higher air velocity through row 6 modules; a decrease in air velocity moving from driver side to passenger side of the modules, with increasing distance from fans; and generally higher air velocity for the top and top middle floors of both row 5 and row 6 modules.

The standard error of estimate was used in order quantify errors from the simulation using a single value. The standard error of estimate was used in a study by Hui et al., (2013) to compare CFD simulated and measured results from an experimental poultry trailer. It can be calculated as follows:

$$\sigma_{est} = \sqrt{\frac{\sum_1^n (Y_{sim} - Y_{exp})^2}{n}}$$

where

$$\sigma_{est} = standard\ error\ of\ estimate$$

$$Y_{sim} = result\ from\ simulation$$

$$Y_{exp} = result\ from\ experiment$$

$$n = number\ of\ data\ points$$

Lower values of standard error of estimate indicate greater agreement with experimental data. The standard error of estimate for air velocity for this simulation was 0.38 m/s, which equated to 32.6% as a percentage of the average velocity

Discrepancy in simulated results and recorded data could be attributed to a range of factors. First, there are possible measurement errors when observing air velocity at a single point within a trailer. As mentioned previously, relatively high values for standard deviation suggest large fluctuations in air velocity in both spatial and temporal dimensions. A small difference in location relative to the fans may result in widely different values for observed air velocity, especially in regions of higher velocity. This study attempted to co-locate the positions of sensors and points monitored in CFD simulations, but it cannot be expected that these points were identical with high exactness. Moreover, operations at a poultry processing plant, such as positioning of fans and trailers as well as fan operation parameters, are rather imprecise. For example, trailer position within holding sheds likely varies with successive trailers in front of the same fan bank. This makes comparing point data for air velocity at the poultry plant and point data from CFD simulation not only difficult, but less useful overall. After data assessment, general trends in air velocity, such as spatial variance as well as relative magnitude, were regarded with more confidence and thus considered more pertinent to this study.

Furthermore, due to time constraints and the difficulty of arranging experimental studies at an operating poultry processing plant, only one experiment trial was completed. The single set of data recorded in this study is most likely insufficient to properly assess conditions on poultry trailers for the purpose of validating the CFD model. A greater array of sensors, as well as replicate trials, may be necessary to accurately characterize conditions within trailer modules

before the CFD model can be validated. A greater array of sensors would also reveal more information on general airflow patterns within poultry modules; these metrics would be more useful to researchers and plant operators, as previously mentioned.

Besides measurement error due to the nature of the system, possible confounding factors for this study included ambient wind and the movement of poultry within modules. Ambient wind was not accounted for in CFD simulation due to its unpredictable and unsteady nature. Ambient wind may be responsible for higher values of air velocity in the bottom floor of row 5 modules than was observed in CFD simulation. In additions, poultry were modeled as a single homogenous mass with certain resistance parameters. This porous media assumption may have led to some error in point data; it is not able to account for possible crowding of birds within modules. Observed point data from plant may be skewed due to this crowding or the presence of a bird directly in front of a sensor. However, the porous media assumption greatly simplified model creation and calculation while preserving the usefulness of the model to predict the aforementioned general trends in air flow through poultry modules.

Geometrical simplifications of the holding shed set up may account for some error as well. Certain small elements on trailer modules, such as the width of support beams and even the unevenness of floors, as well as the poultry trailer itself, were not included in CFD simulation, and may indeed have significant effect on airflow. In addition, space behind modules was left empty in CFD simulation. At the processing plant, this space is intermittently occupied by a second trailer or left empty. Also present is a second row of fans, directly opposite the row modeled and intended to provide airflow over modules in the second trailer. It is possible, especially when a second trailer is not present, that airflow from this second set of fans reaches

the passenger side of trailer modules. This could account for higher values of observed air velocity for the passenger side of some modules.

In conclusion, simulated data agreed reasonably well with experimental data, and CFD simulation was able to replicate some of the expected trends in airflow, such as higher air velocity near fans and in row 6 modules. However, due to the paucity and nature of the data, the CFD model may not yet be considered "validated" by some. However, it should be mentioned though that there is no single accepted standard in order for a CFD model to be considered "accurate." Rather, the usefulness of the CFD model, as well as the degree of validation necessary, is contingent upon the needs of the user.

4.3 Airflow Visualization

From CFD simulated data, contour plots of velocity and streamlines were created in ANSYS Fluent. Figure 4.3 indicates the location of contour planes in figure 4.4. Contours were created both parallel to the axis of the fan and perpendicular to the axis of the fan to show variation in air velocity with increasing distance from the fan as well as lateral variation within the modules.

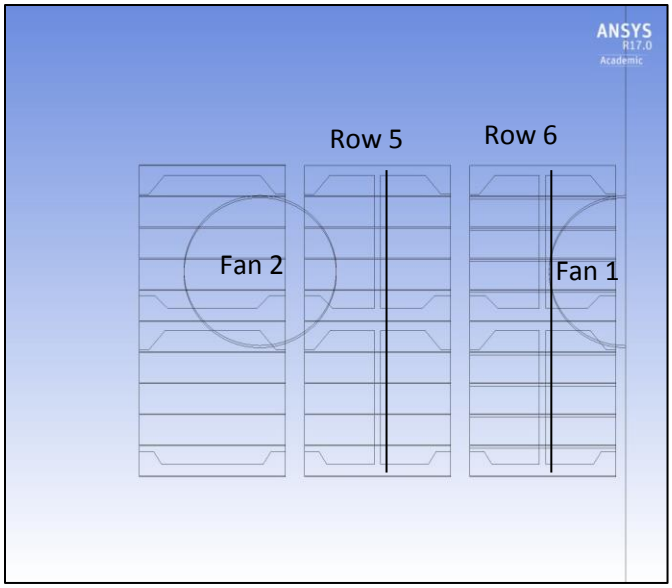

Figure 4.3: Specification of rows 5 and 6 and fans 1 and 2. Vertical lines indicate location of planes in figure 4.4

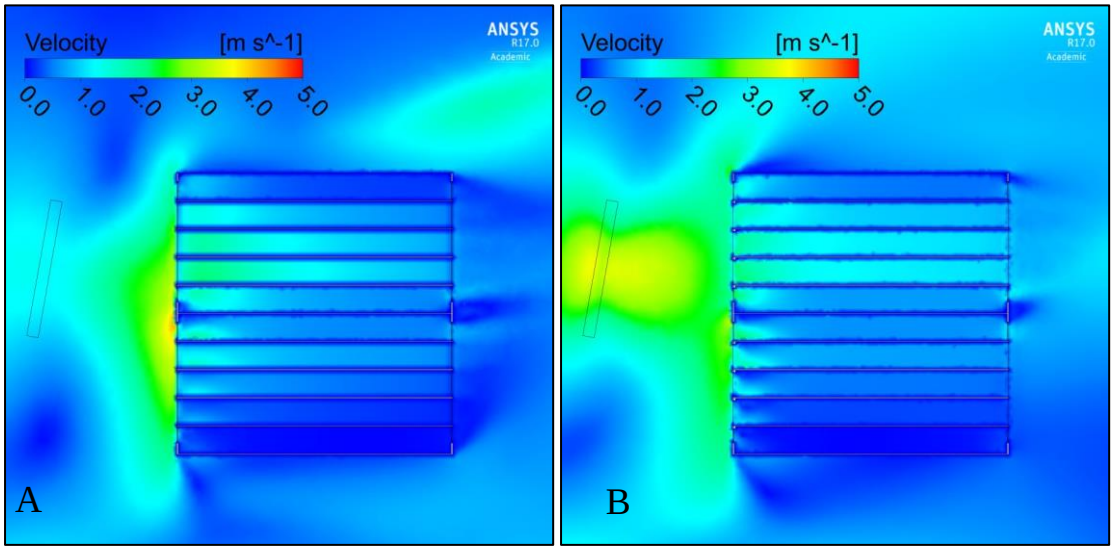

Figure 4.4: Contours of velocity magnitude for cross sections in middle of row 5 (A) and row 6 (B)

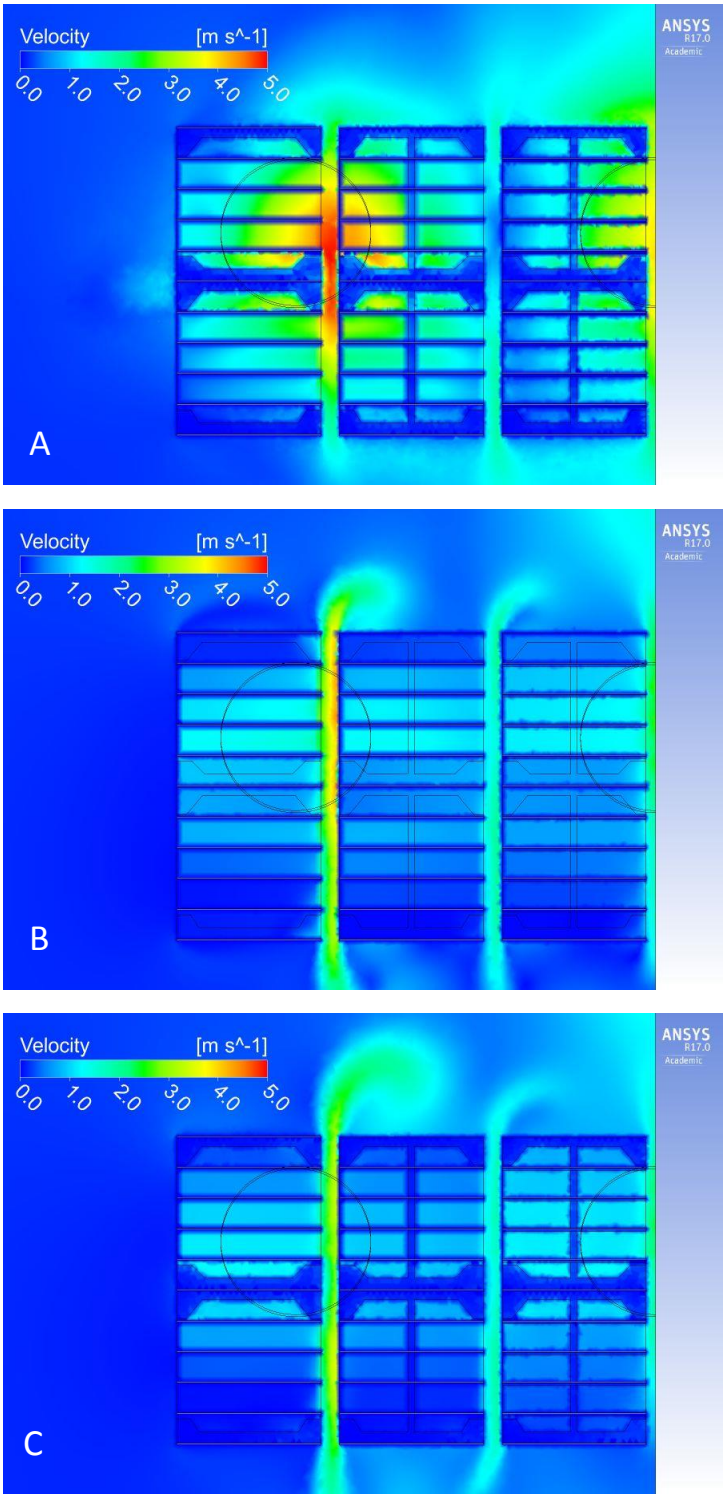

Figure 4.5: Contours of velocity magnitude for cross sections with increasing distance from the fan. Plane (A) is positioned 0.025 m from the fan side of the modules within the modules; (B) is positioned 1.22 m from the fan side of the modules, exactly halfway in this direction; (C) is positioned towards the rear of the modules, 0.025 m from the far side of the modules.

These results show general trends for air velocity patterns within trailer modules. Figure 4.4 suggests the importance of module-fan alignment with respect to airflow within modules. First, for the cross section in row 6, airflow immediately in front of the fan shows a similar profile to inlet velocity from the fan. As air comes into contact with the front faces of the modules, a significant amount is deflected. Air that does enter the modules decreases in velocity as it moves toward the back of the modules, similar to trends in experimental data.

In contrast to the plane in row 6, the cross section in row 5 experienced much less airflow penetration into the module due to not being in a plane in line with any point on the faces of either fan. Again, the trend of decreasing velocity with increasing distance from the fans is repeated for air in this plane. A small area with high velocity is noticed in front of the module in face in row 5. Most likely, this air has a large velocity component in the direction normal to the cross section; it can be seen that this air velocity is not transferred to the interior of the module. Finally, for planes in both rows 5 and 6, there was a large discrepancy of airflow between regions separated vertically. Again, this is most likely a function of less air going into module regions not aligned with the faces of fans; in this case, these were the uppermost and bottommost floors. Especially for the bottommost floors, air had a large downward vertical component after being deflected from the faces of the modules, causing less air to actually flow into the modules.

Figure 4.5 shows lateral variation in airflow within modules. Near the front face of the modules experiencing airflow, there was large spatial variation corresponding to placement of the fan; airflow at the front face of the module seemed to have a shape similar with the shape of the fan. With increasing distance from the fans, lateral variation in air velocities decreased; within a specific floor, air velocity was rather homogenous for planes at distances midway from the front face of the modules and near the back of the modules. It can be assumed that not only

did a fraction of the air from fans enter modules, but this air was deflected as well and given some component of velocity not parallel to initial airflow. This may explain the relative homogeneity of air velocity with increasing distance from fans; with increasing distance from the fan, air became more dispersed and had less velocity magnitude.

The effect of doors was minimal on local air velocities; there is nothing remarkable about airflow in close proximity to doors. Of final note in figure 4.5 is the relatively high velocity for air within the gaps between modules. It can be assumed that a large amount of air was directed into this space as it poses no resistance to airflow and the width of the gap is large enough that drag created by the surface of the doors is not significant to deter flow. This air that travels between modules may essentially be considered wasted; it represents an amount of energy input that does nothing to cool birds within modules. Furthermore, air velocity in the gap between modules did not decrease to the same degree with increasing distance from fans. The Venturi effect may contribute to this result, causing air velocity necessarily to increase with a decrease in area. The problem of air travelling between modules may be simple to solve; design alternative 2 in section 4.5 explores a method to decrease the airflow through the gap between modules.

The ability to create streamlines of air velocity is another advantage of CFD simulation difficult to replicate in experimental studies. Figure 4.6 gives further insight into flow patterns of air from the fans and through modules. As surmised previously, figure 4.6 shows a portion of the air from fans was deflected before entering into modules. Some of the deflected air was also brought back into the intakes of the fans. Additionally, air that did enter the modules was deflected and velocity magnitude reduced greatly.

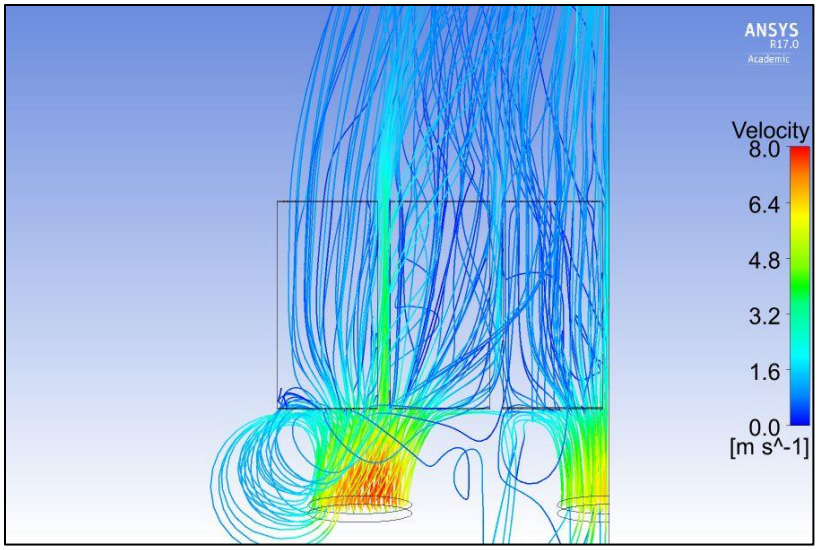

Figure 4.6: Streamlines of airflow from both fans: aerial view

Figure 4.7 isolates streamlines within modules. From figure 4.7, a large portion of air in row 5 modules had a diagonal component and exited through the sides of modules opposite the doors. Also noticeable was the area in close proximity to the doors in row 5 modules that received little airflow. In contrast, more airflow in row 6 modules had direction toward the back face of modules and was distributed more evenly throughout the modules.

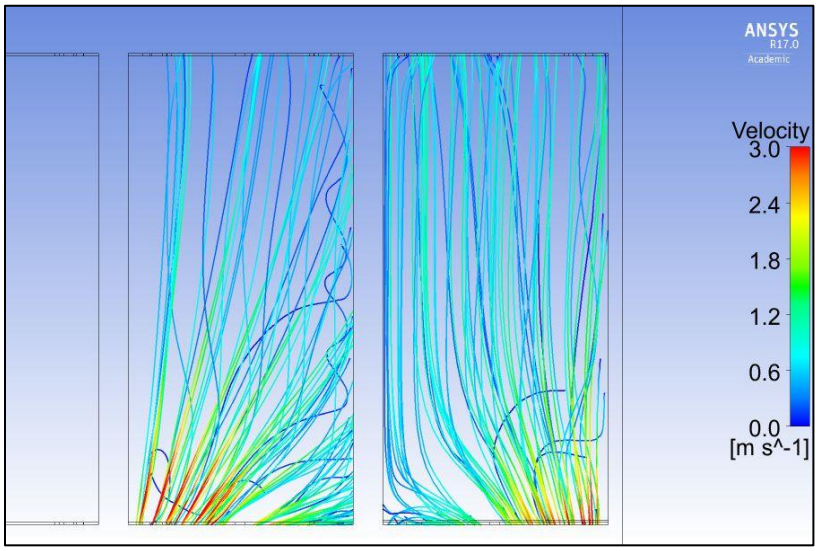

Figure 4.7: Aerial view of streamlines released from front face of modules, colored for velocity

Table 4.6: Airflow traveling through trailer modules

Trailer Region	Mass Flow Exit Through Back (kg/s)	Percentage of Mass Flow into Domain Through Modules
Row 5 Modules	1.52	13.1%
Row 6 Modules	2.15	18.5%
Mass Flow Rate from Fans (kg/s)	11.61	

Visualization of results suggested that a large amount of air from the fans did not actually enter into or travel through the length of poultry modules. To quantify this amount and to judge the relative performance of the holding shed cooling strategy, mass flow rate from the fans as well as mass flow exiting the back of each row of modules was calculated. Table 4.6 shows a large difference in mass flow of air exiting the back faces of modules in row 5 compared to row 6. This was previously attributed to the positioning of each row of modules relative to the two fans; a larger amount of air from the first fan is incident on row 6, while fan 2 is positioned off center from the centerline of row 5. While movement of a fan slightly off the center axis of modules may seem minor, these results quantify the difference. The effects of an off-center fan could indeed be significant; airflow rate from CFD simulation through row 6 modules was approximately 41.4% higher than airflow through row 5 modules. Interesting to note is that only 13.1% and 18.5% of air mass from the fans travelled through row 5 modules and row 6 modules, respectively. If simulations are indeed a reasonable indication of airflow at poultry holding sheds, then it can be seen that a large portion of air does not travel into and through modules, and has no cooling effect on birds within.

4.4 Sensitivity Analysis Results and Standard Error of Estimate

Results from the separate simulations in the sensitivity analysis are displayed in table 4.7. First, it should be mentioned that these results were not tested for significance. Variations in results could be due in part to calculation error.

Table 4.7: Results from sensitivity analysis

Simulation	Description	σ_{est} (m/s)	Max. Velocity (m/s)	Avg. Velocity (m/s)
Default	Fan Pressure = 47.2 pa, AOZ viscous resistance = 57,755	0.38	2.3	1.0
Fan Condition 1	Fan Pressure=41.5 pa	0.43	2.6	0.9
Fan Condition 2	Fan Pressure=54.5 pa	0.44	3.1	1.0
Fan Condition 3	Fan Pressure=80.5 pa	0.54	3.6	1.2
AOZ Condition 1	AOZ viscous resistance = 20,000	0.49	3.1	1.0
AOZ Condition 2	AOZ viscous resistance = 40,000	0.48	3.0	1.0
AOZ Condition 3	AOZ viscous resistance = 80,000	0.45	2.6	0.9

Changes in fan pressure condition led to expected changes in air velocities within poultry modules. In general, air velocity decreased for monitored points when fan pressure was decreased to 41.5 pa. Conversely, air velocity increased for nearly all monitored points when fan pressure was equal to 54.5 pa, and increased further when fan pressure was equal to 80.5 pa. Notable is that maximum air velocity actually increased when fan pressure was decreased for fan condition 1. This variation, measured at the fan side of the top middle floor of row 6 modules, is most likely due to calculation error; as mentioned, this variation may not be significant. When all points are considered, average velocity for fan condition 1 was 0.9 m/s compared to 1.0 m/s for the default simulation.

The lowest value of standard error of estimate was observed when fan pressure was 47.2 pa in the default condition. However, when considering the appropriate boundary condition to use, air velocities at the front face of modules may be most indicative of accurate inputs for fan conditions. The input fan condition serves only to increase the pressure of air moving through the fan domain. Once air flow exits the fan outlet, its trajectory is dependent more on the surrounding geometry, porous media conditions within the modules, and other boundary conditions. Though the default fan condition resulted in the lowest standard error of estimate, a more thorough procedure of model calibration may improve upon methods used in the default simulation. While the default simulation used factory specifications from a typical fan of the same model and size employed at the test site, it was not confirmed that the fans used in experimental tests were operating at these specifications. In fact, it should be expected that fans in use at poultry processing plants do not operate at factory specifications; it is more likely that they operate at lower performances due to wear and tear.

Separate conditions for the viscous resistance coefficient in the porous media zone were also tested to assess the sensitivity of the model to this parameter. Within Fluent, the porous media zone acts as a momentum sink for moving fluids. Decreases in resistance coefficients should increase the velocity of air in the porous media. In a sense, this can also be considered an evaluation of the accuracy of the sub-model method used to determine resistance parameters for the porous media zone, since the baseline parameters were chosen empirically using this method.

Reductions in the viscous resistance coefficient in the AOZ led to expected changes in airflow velocity. Maximum velocity, which was observed at the fan side area of row 6 modules, increased from 2.3 m/s to 3.1 m/s and 3.0 m/s for AOZ condition 1 and AOZ condition 2, respectively. Average velocity of all points measured did not vary substantially between default

simulations and both AOZ condition 1 and AOZ condition 2. Conversely, average air velocity within modules decreased for AOZ condition 2, which had a higher viscous resistance coefficient than default simulations. Standard error of estimate increased for all three AOZ alternative conditions, lending credence to the use of the porous media sub-model to determine accurate resistance parameters in the porous media zone.

4.5 CFD Simulation of Alternative Holding Shed Strategies

An objective of this study was to develop a CFD model with the ability to test various holding shed cooling strategies and use the results to reliably inform decisions that poultry producers make in the future. Changes in cooling strategies in holding sheds could range from relatively simple, such as placement of modules and fans, to complex, such as a system to funnel air into the poultry modules. Three hypothetical design alternatives were considered. Testing these design alternatives served multiple purposes: it established how easy it was to adjust the model to various holding shed cooling strategies, it showed how the model reacted to changes in geometry and boundary conditions, and it identified some possible changes in holding shed design that could potentially improve air velocity through poultry trailers. Design alternatives tested in this study are described in Table 4.8.

Table 4.8: Description of design alternatives

Design Alternative	Description
Design Alternative 1	Decreased gap width between adjacent module rows
Design Alternative 2	One fan per module row set up (42 in. diameter fan, centrally aligned with row)
Design Alternative 3	Enclosure to direct flow into modules

Results from design alternatives are quantified in terms of air velocities within poultry modules. In general, higher air speeds are desired during warm conditions. However, quantifying the actual effect on poultry welfare of increasing air velocity a certain degree was not considered in this study. Furthermore, when considering these design changes, poultry plant operators need to weigh the potential benefits of design changes to the capital and operating cost of these design changes. These factors were not considered in this study.

4.5.1 Design Alternative 1

Velocity contours in figure 4.5 suggested that a considerable amount of air from the cooling fans traveled between modules, representing a possible loss in potential air velocity and its concomitant cooling effect within the modules. The distance between stacks of modules was measured as approximately 0.15 m (6 in.). In design alternative 1, a small modification was made to the CFD model by moving stacks of modules nearer to each other, decreasing the spatial gap between them to 0.05 m (2 in.). All other model parameters, including boundary conditions and solution methods, were kept the same.

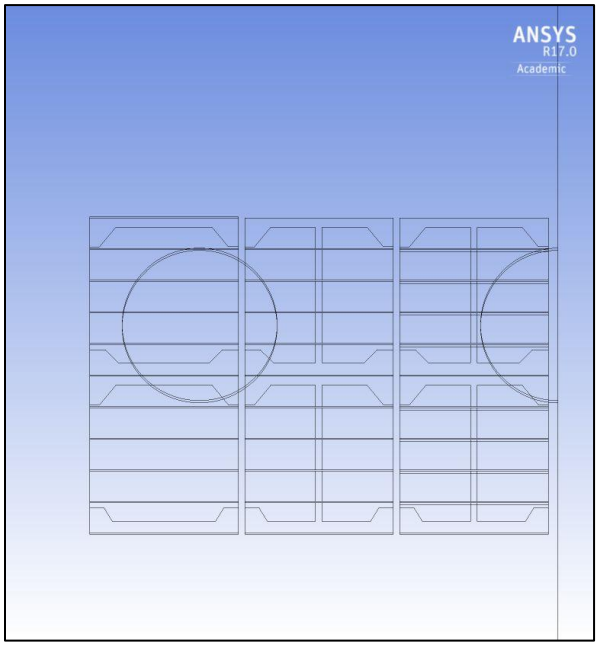

Figure 4.8: Geometry of design alternative 1

Volume percentage graphs show the relative portion of volume within the module spaces with a certain velocity range. For example, approximately 10 % of the air volume within the module space had velocity 1 – 1.25 m/s, for both design alternative 1 and the baseline scenario. The results for the default holding shed design (termed "baseline") are superimposed on those of design alternative 1 in figure 4.9. It should be mentioned that standards for acceptable airflow through poultry modules in a holding shed are not well defined. Bird welfare is affected by a combination of related factors including local air velocity, temperature, and relative humidity (Tao and Xin, 2003). Therefore, these results cannot be used to determine the effect that various design alternatives would have on bird welfare in holding sheds, and whether or not it is significant and worth the potential cost of the design alternative. However, higher air velocity is positively correlated with an increased cooling effect; all other things equal, higher velocity within the module space during warm conditions is desired. Figure 4.9 shows design alternative 1 increased slightly the amount of air with velocity greater than 0.5 m/s, and decreased slightly the amount of air with velocity less than 0.25 m/s.

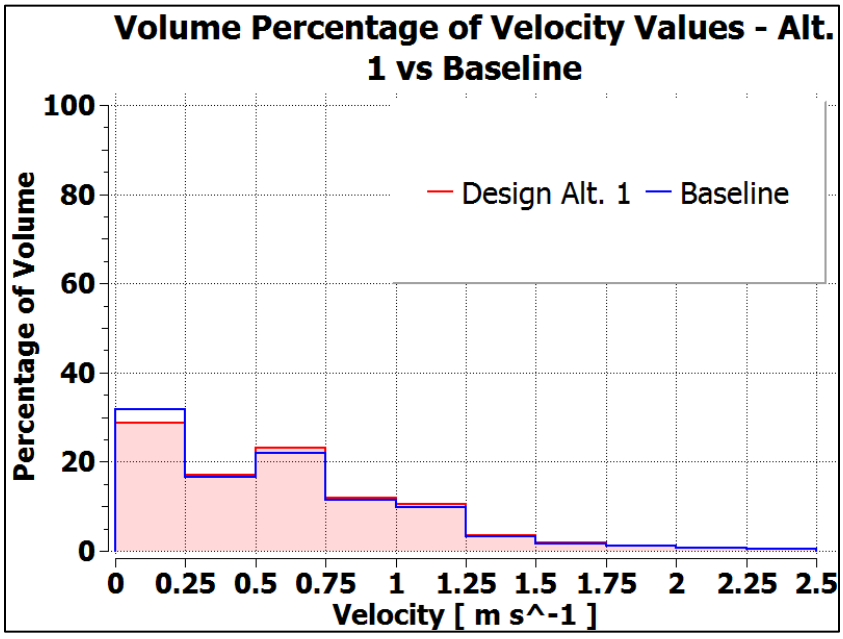

Figure 4.9: Volume percentage of velocity values within row 5 and 6 modules – design alternative 1 vs baseline scenario

Furthermore, table 4.9 shows that row 5 and row 6 modules were not affected equally; row 5 modules experienced a 9.9 % increase in mass flow exit through the back face, while there was no noticeable difference for row 6 modules. The reason for this may be that while the gap space between row 5 and row 6 modules was decreased in design alternative 1, the gap space between row 6 modules and the symmetry plane was not. Even so, these results indicate that closer placement of modules is perhaps beneficial to airflow through the interior space. However, results in figure 4.9 and table 4.9 were not tested for significance. Also not considered is the effect that closer placement of modules may have on airflow through modules during transit of the poultry trailers from farm to processing plant.

Table 4.9: Comparison of mass flow exit through back of poultry modules

Trailer Region	Mass Flow Exit Through Back (kg/s)	Percent Change from Base Scenario
Row 5 Modules	1.52	-
Row 6 Modules	2.15	-
Row 5 Modules (Alt. 1)	1.67	+9.9 %
Row 6 Modules (Alt. 1)	2.15	0 %

4.5.2 Design Alternative 2

Results from the baseline scenario, in addition to experimental data, suggested that row 5 modules as well as modules positioned on the bottom of each row received less airflow, most likely due to being misaligned with either fan axis. It was hypothesized that a holding shed strategy using one fan per row of modules and aligned with the center of each row of modules would deliver greater and more homogenous airflow. Design alternative 2 tested this

hypothesis. The geometry consisted of an additional fan; each fan was positioned at the center of one row of modules. In addition, the diameter of each fan was 1.07 m (42 in.), compared to 1.22 m (48 in.) in the baseline scenario. The fans were also given a 90° vertical mounting angle, compared to the 10° downward tilt of the fans in the baseline scenario.

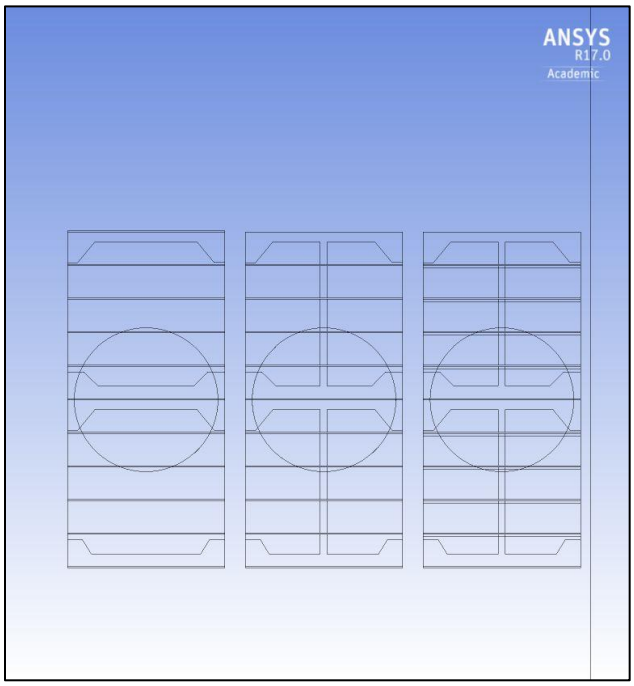

Figure 4.10: Geometry of design alternative 2

A volume percentage graph of velocity values shows the relative amount of air with velocity greater than or equal to 1.25 m/s was increased in design alternative 2. The percentage of air with velocity less than 0.25 m/s remained the same, while air with velocity 0.5-1.0 m/s was greatly reduced. Figure 4.11 accounts for all air within row 5 and row 6 modules. To see how airflow is distributed, it is necessary to separately examine row 5 and row 6 modules, as well as the top and bottom cages in each of these rows.

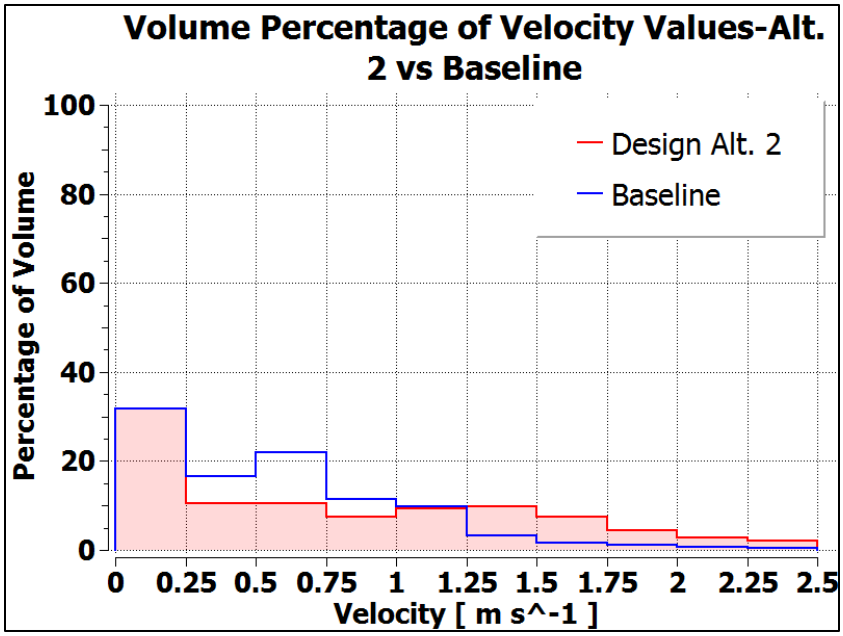

Figure 4.11: Volume percentage of velocity values within row 5 and 6 modules – design alternative 2 vs baseline scenario

Figure 4.12 shows that design alternative 2 greatly increased airflow velocity in the bottom cage of row 5 modules, likely an effect of the lowered position of the fan. Airflow through the top cage of row 5 modules was also improved, however to a lesser degree, with an increased volume of air with velocity greater than 1.0 m/s. Relative to the baseline scenario, row 6 modules experienced less benefit from design alternative 2. For design alternative 2, bottom cages on row 6 had a larger portion of air with velocity over 0.75 m/s, while top cages in row 6 had a noticeable increase in air with velocity less than 0.25 m/s. It can be concluded that design alternative 2 increased homogeneity of airflow through adjacent rows of modules, but increased the discrepancy in sections of the poultry trailer separated vertically.

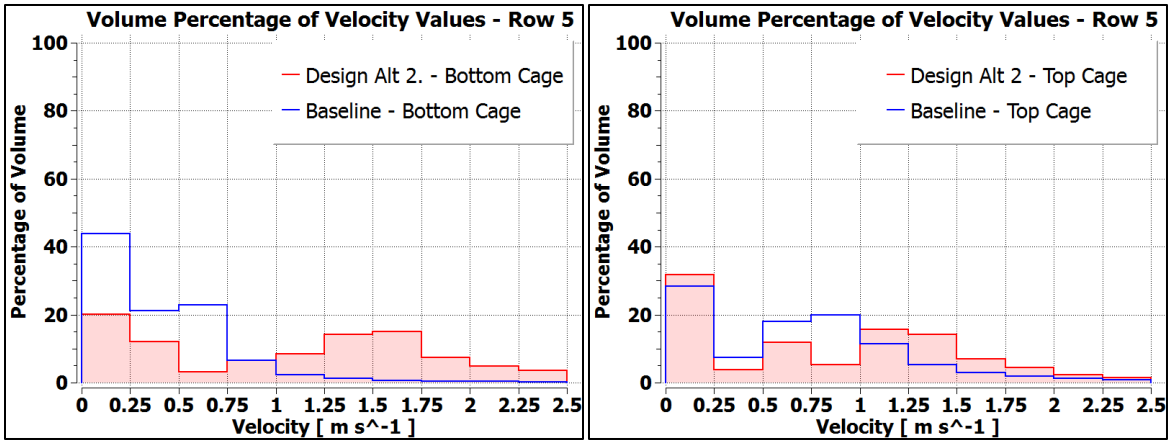

Figure 4.12: Comparison of volume percentage of velocity values for top and bottom cages: row 5 modules

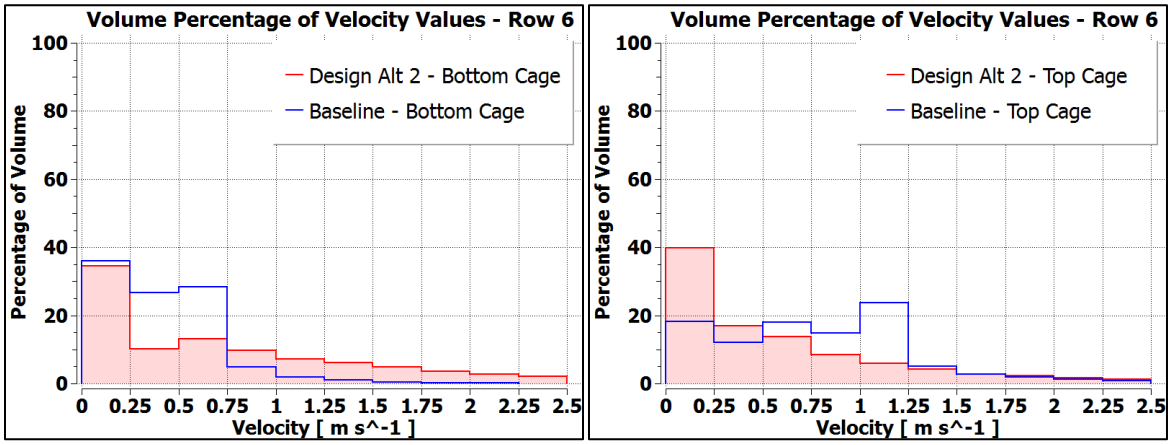

Figure 4.13: Comparison of volume percentage of velocity values for top and bottom cages: row 6 modules

These results suggest that central placement of fans in a one fan per module row configuration is not ideal for adequate and homogenous airflow through all sections of the poultry trailer. However, it was apparent that each row of modules will benefit from having a fan of its own, as evidenced by the increased airflow in row 5 modules, and to a lesser extent row 6 modules, relative to the baseline scenario, as shown in table 4.10. If a one fan per module row configuration is used, the ideal placement of this fan is most likely similar to that seen in the baseline scenario and at the test site, where the fan is positioned higher and with a slight downward tilt. An additional fan, creating a two fans per module row configuration, may also increase performance and could be worth testing.

Table 4.10: Comparison of mass flow exit through back of poultry modules

Trailer Region	Mass Flow Exit Through Back (kg/s)	Percent Change from Base Scenario
Row 5 Modules	1.52	-
Row 6 Modules	2.15	-
Row 5 Modules (Alt. 2)	3.08	+ 102.6%
Row 6 Modules (Alt. 2)	3.05	+ 41.9%

4.5.3 Design Alternative 3

Design alternative 3 proposed a method to channel air into the interior space of modules, increasing the cooling efficiency of fans. By using some form of enclosure or baffle surrounding the airspace between the fan and the module, air exiting the fan would be forced into the face of the modules. This setup would require that each row of modules have a separate fan. Furthermore, it cannot be expected that the output from similar fans would be the same in this system. The enclosure would increase the system pressure on the fan, decreasing flow rate from the fan.

A higher degree of modification to the baseline model was needed in order to test design alternative 3. These changes involved the geometry as well as boundary conditions. Only one row of modules was included in the simulation of design alternative 3, since each fan-module system would be isolated from the others. Otherwise the position and size of the fan used was similar as the fan in design alternative 2. A rectangular enclosure was made that stretched from the inlet face of the fan to the front face of the modules, with height equal to one row of modules. The space between the fan and module was thus enclosed, so airflow from the fan had no outlet but through the front face of modules. Figure 4.14 shows the geometry of design alternative 3.

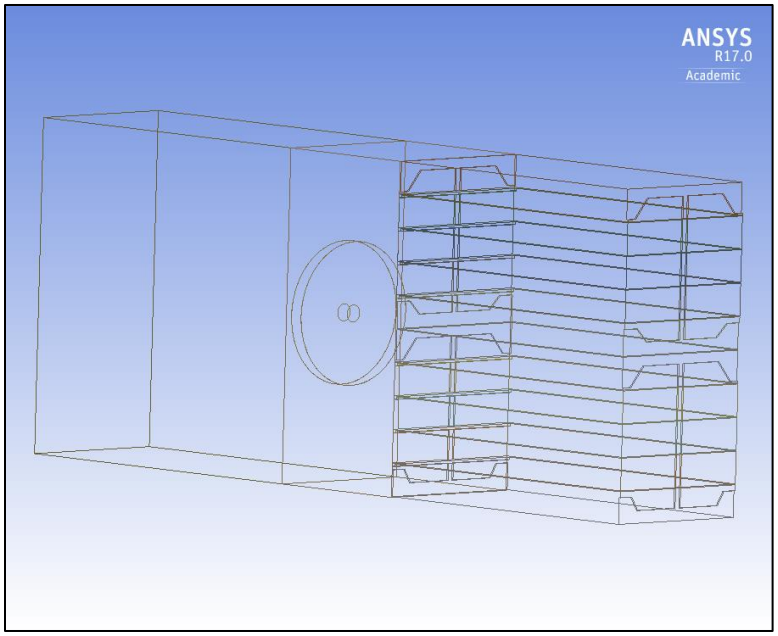

Figure 4.14: Geometry of design alternative 3

As before, one side of the module faces was designated as doors with boundary condition "wall." However, it was less clear how to designate the sides of the modules opposite the doors. The flow through these faces is open to the atmosphere, but it is inhibited somewhat by the proximity of adjacent modules. Neither an open pressure outlet condition nor a sealed "wall" condition would be totally accurate. To compromise, a pressure outlet condition with gauge pressure 5 pa was used. This value was approximately equal to the average pressure observed at the module faces opposite to the doors in design alternative 2, which had similar geometry to design alternative 3.

Previously, a constant pressure rise for the fan had been used in all simulations. However, the presence of a baffle enclosure would have large effects on the system pressure, and it is unreasonable to assume that fan output would remain the same as previous model iterations. As before, the 3D fan model within ANSYS Fluent was used to model the fan zone; however, the pressure rise for this simulation was specified using a fan curve. By using fan curve data, Fluent

automatically calculates flow rate from the fan based on the pressure of the system. A fan curve of a typical fan used in a poultry trailer holding shed was implemented into the model.

Design alternative 3 created a noticeable shift toward higher velocity values compared to the baseline scenario. The volume of air with velocity less than 0.25 m/s was reduced significantly, most likely corresponding to regions toward the back of the modules. In addition, there was a substantial increase in airflow with velocity greater than 1 m/s.

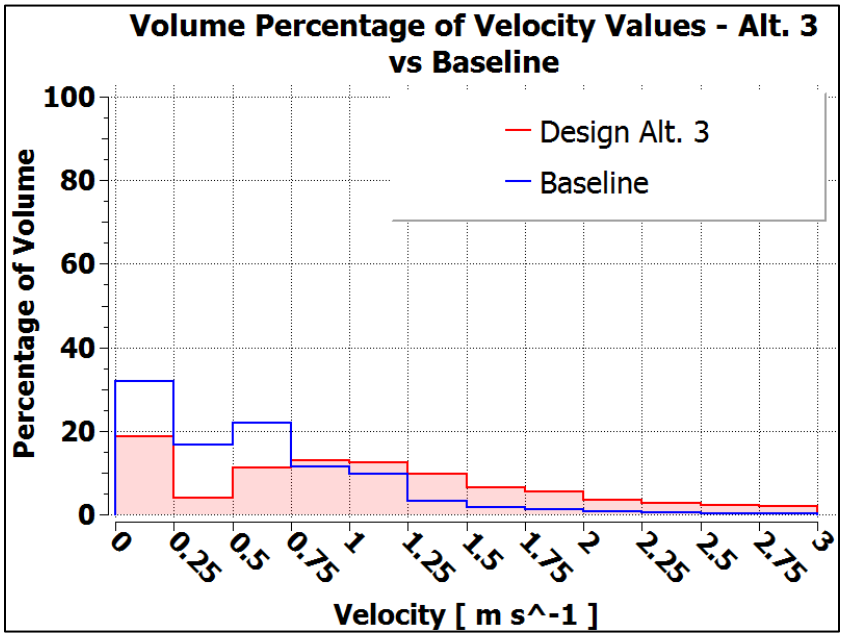

Figure 4.15: Volume percentage of velocity values – design alternative 3 vs baseline scenario, average of row 5 and row 6 modules

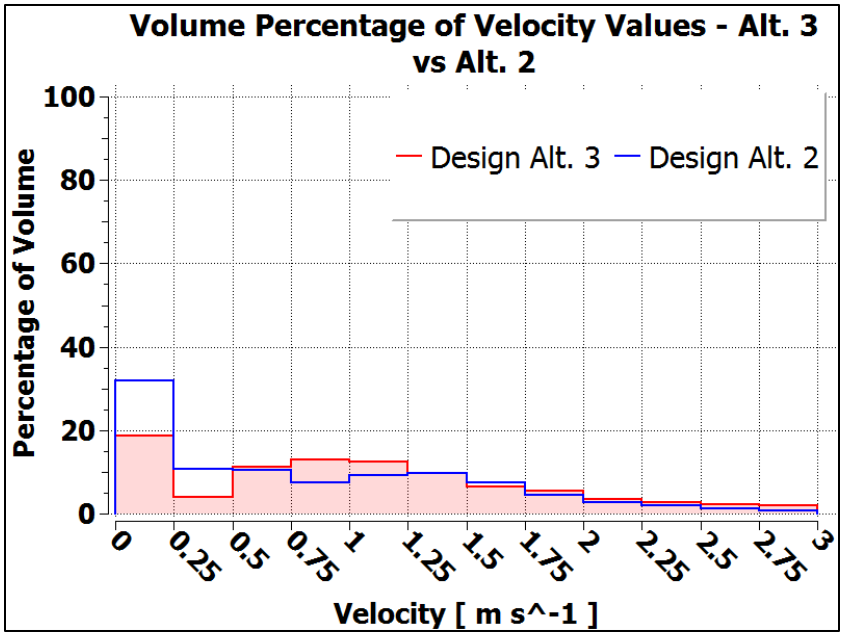

Figure 4.16: Volume percentage of velocity values – design alternative 3 vs design alternative 2

Compared to design alternative 2, which had similar geometry, design alternative 3 had a 1.38 kg/s increase in air flow rate through the back of modules, or approximately 44.8%. This improvement can be attributed to the presence of the baffle in design alternative 3 forcing air into the front face of modules. However, uncertainty in the boundary condition of module faces opposite the doors gives less confidence to the flow rate value calculated. Future testing may be needed to specify this boundary condition with more confidence. Regardless, it would be expected that this system would improve airflow through the interior of poultry modules, and these results were observed in the simulation.

Table 4.11: Comparison of mass flow exit through back of poultry modules

Simulation	Mass Flow Exit Through Back (kg/s)	Percent Change
Design Alternative 2	3.08	-
Design Alternative 3	4.46	+44.8%

Contours of velocity magnitude in a middle cross section elucidate some of the observed differences due to the addition of a baffle in design alternative 3. Airflow from the fan in design alternative 2 is deflected upon reaching the module faces. A large portion of the air does not penetrate into the modules, travelling both above and beneath them. Airflow through the bottom floors in design alternative 2 is also greater than airflow through the top floors.

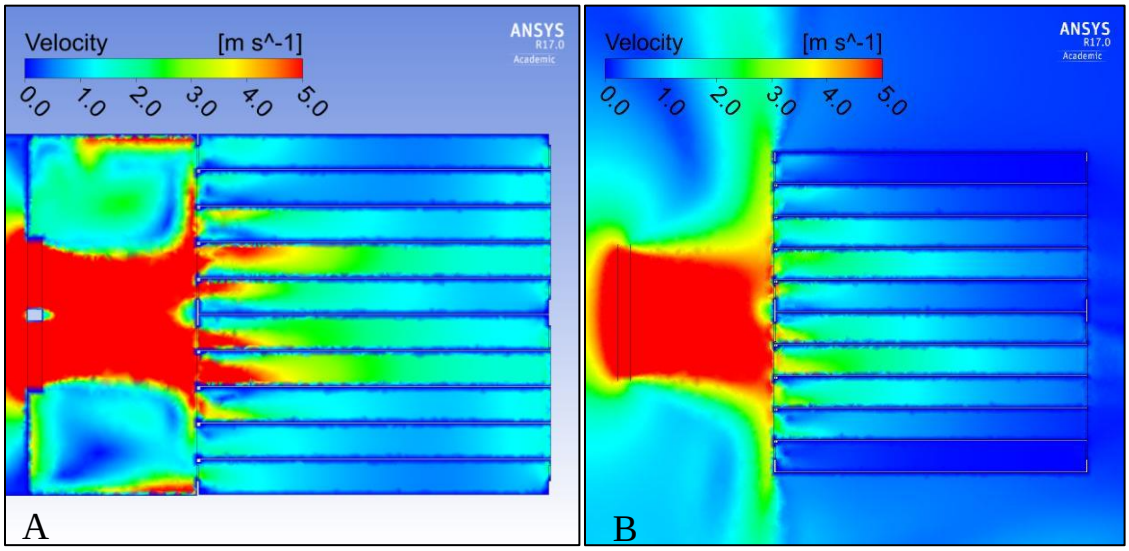

Figure 4.17: Contours of velocity magnitude for middle cross sections in design alternative 3 (A) and design alternative 2 (B)

In contrast, airflow from the fan in design alternative 3 is necessarily forced into the module, causing increased velocity in all sections. Additionally, airflow is more homogenous in nature. Since the baffle encloses the space from the top and bottom as well, air reaching the top and bottom floors that normally has large upward or downward component and does not penetrate into the modules is deflected by the baffle and is forced into the interior of these sections. Airflow velocity is still largest for the sections positioned directly downstream from the fan exhaust. However, there are no sections of the module in the middle cross sections that do not experience increased airflow. While design alternative 3 may be most difficult to implement

at poultry processing plants, results suggest that it could greatly improve airflow through poultry modules.

5. Conclusions and Recommendations

In this study, a CFD model for simulating conditions within a loaded poultry trailer in a simple holding shed configuration was created. All aspects of model construction, including geometry and mesh creation, specification of model and solution parameters, and solution of the flow field, was done using the commercial CFD package ANSYS Fluent. In addition, experimental data was collected from within a poultry trailer situated in a holding shed during warm summer conditions. This data was used as a reference point to assess simulation results.

One of the initial objectives of this study was to create a validated CFD model that could be used to test alternative cooling strategies within holding sheds and use model results to inform decisions made by poultry processors. The author would be hesitant to recommend the CFD model for use in industry in its current form however. There are a number of areas of uncertainty, both in model parameters and the experimental data collection process, that are difficult to ignore. It is questionable whether the method of collecting point data for air velocity within poultry trailers is the ideal process for validation of the CFD model. Practices in poultry trailer holding sheds, along with data acquisition methods, are by nature imprecise; fans and trailer placements, as well as fan performance, are inexact. This most likely makes model calibration for specific settings necessary. In addition, the locations of chickens within the module are transient and not well defined, and can disrupt collection of air velocity data. Therefore, it is unreasonable to predict with much confidence the small spatial variations in temperature, humidity, and air velocity within poultry trailers. Rather, knowledge of the magnitude and spatial trends of these parameters is more relevant. A more robust series of

experiments, including additional sensors and replicate trials, would give researchers more confidence in knowledge of airflow characteristics within poultry trailer holding sheds. A scale model may even possibly be useful for validation of CFD model, as is seen in Gilkeson et al. (2009). In addition, experimental data for a variety of different holding shed configurations is of need to further test the CFD model's accuracy in different settings. Further sensitivity analysis of the completed CFD model is also necessary, including analysis of the effect of turbulence model and solution methods, as well as a mesh convergence study.

While the accuracy and the degree of validation performed in this study may not be acceptable for some applications, preliminary results from this study showed that CFD simulation has potential usefulness in future studies. Results of point data for air velocity were of the same magnitude as those observed in the experimental study. General spatial trends in air velocity data were replicated in simulations. This leads credence to the use of porous media as a method to model the animal occupied zone; this practice has potential application in a wide range of research. Furthermore, as seen in section 4.5, CFD simulations showed the ability to respond to certain design changes and produce results, though not verified, that seem reasonable. Indeed, it is this ability to efficiently test design alternatives that is one of the major attractions of CFD in this research field.

Further advantages of the CFD simulations included examination of air velocity at any point in the model domain, both in and around poultry trailers. This facilitated the creation of contour plots in multiple domains, as well as streamlines to visualize airflow. This information could allow researchers to identify areas of high and low velocity within poultry trailers that may go unnoticed in experimental studies.

Future research involving application of CFD to poultry trailer holding sheds could build upon this study in a number of ways. As mentioned, most important is a more robust system of calibration and validation of the CFD model. Incorporating temperature and humidity into this model while accounting for heat and moisture production of birds is a logical addition. Modeling these parameters would greatly increase the usefulness of the CFD model to assess the impact of cooling shed strategies on bird welfare. If these parameters are implemented, and a suitable and more robust method for validation of the CFD model can be achieved, the CFD model could be a valuable tool for improving conditions for live animals within poultry trailer holding sheds.

References

Aerts, J., & Berckmans, D. (2004). A Virtual Chicken For Climate Control Design: Static And Dynamic Simulations Of Heat Losses. *Transactions of the ASAE, 47*(5), 1765-1772.

ANSYS Fluent Features. (n.d.). Retrieved October 7, 2015, from http://www.ansys.com/Products/Simulation Technology/Fluid Dynamics/Fluid Dynamics Products/ANSYS Fluent/Features

Arkansas Poultry | Broilers, Turkeys, Chicken Egg Production. (n.d.). Retrieved October 7, 2015, from http://www.uaex.edu/farm-ranch/animals- forages/poultry/

Blanes-Vidal, V., Guijarro, E., Balasch, S., & Torres, A. (2008). Application of computational fluid dynamics to the prediction of airflow in a mechanically ventilated commercial poultry building. *Biosystems Engineering, 100*(1), 105-116.

Bustamante, E., García-Diego, F., Calvet, S., Estellés, F., Beltrán, P., Hospitaler, A., & Torres, A. (2013). Exploring Ventilation Efficiency in Poultry Buildings: The Validation of Computational Fluid Dynamics (CFD) in a Cross-Mechanically Ventilated Broiler Farm. *Energies, 6*(5), 2605-2623. doi:10.3390/en6052605

Dalley, S., Baker, C., Yang, X., Kettlewell, P., & Hoxey, R. (1996). An Investigation of the Aerodynamic and Ventilation Characteristics of Poultry Transport Vehicles: Part 3, Internal Flow Field Calculations. *Journal of Agricultural Engineering Research, 65*(2), 115-127.

Dozier, W. A., Lott, B. D., & Branton, S. L. (2005). Growth responses of male broilers subjected to increasing air velocities at high ambient temperatures and a high dew point. *Poultry Science, 84*(6), 962-966.

Gilkeson, C., Thompson, H., Wilson, M., Gaskell, P., & Barnard, R. (2009). An experimental and computational study of the aerodynamic and passive ventilation characteristics of small livestock trailers. *Journal of Wind Engineering and Industrial Aerodynamics, 97*(9-10), 415-425. doi:10.1016/j.jweia.2009.06.004

Gilkeson, C., Thompson, H., Wilson, M., & Gaskell, P. (2016). Quantifying passive ventilation within small livestock trailers using Computational Fluid Dynamics. *Computers and Electronics in Agriculture, 124,* 84-99. doi:10.1016/j.compag.2016.03.028

Hoxey, R., Kettlewell, P., Meehan, A., Baker, C., & Yang, X. (1996.). An Investigation of the Aerodynamic and Ventilation Characteristics of Poultry Transport Vehicles: Part I, Full-

scale Measurements. *Journal of Agricultural Engineering Research, 65*, 77-83.

Huffman, H. (2000). Tunnel ventilation for livestock and poultry barns. Fact Sheet 00-085. Ontario Ministry of Agriculture, Food and Rural Affairs. Ontario, Canada.

Hui, K. C. (2013.). Development and Evaluation of an Actively Heated and Ventilated Poultry Transport Vehicle. PhD dissertation. Saskatoon: University of Saskatchewan, Department of Chemical and Biological Engineering

Kacira, M., Short, T., & Stowell, R. (1998). A Cfd Evaluation Of Naturally Ventilated, Multi-Span, Sawtooth Greenhouses. *Transactions of the ASAE, 41(3),* 833-836.

Kettlewell, P., Hoxey, R., & Mitchell, M. (2000). Heat produced by Broiler Chickens in a Commercial Transport Vehicle. *Journal of Agricultural Engineering Research, 75*(3), 315-326.

Kettlewell, P., Hoxey, R., Hartshorn, R., Meeks, I., & Twydell, P. (2001). Controlled ventilation system for livestock transport vehicles. Livestock Environment VI, Proceedings of the 6th International Symposium 2001.

Luthra, K., Y. Liang, J. R. Andress, T. A. Costello, S.E. Watkins, D. Aldridge. 2018. Construction and Performance of a Self-Contained, Temperature-Controlled Heat Source (Electronic Chicken) to Quantify Thermal Load During Live Haul of Broilers. *Applied Engineering in Agriculture*. In Revision.

Liang, Y., Liang, Z. (2015). Monitoring Thermal Environment on a Live Haul Broiler Truck. ASABE Annual International Meeting Presentation. Paper Number: 152189918, ASABE, St. Joseph, MI

Norton, T., Sun, D., Grant, J., Fallon, R., & Dodd, V. (2007). Applications of computational fluid dynamics (CFD) in the modelling and design of ventilation systems in the agricultural industry: A review. *Bioresource Technology, 98*(12), 2386-2414.

Norton, T., Grant, J., Fallon, R., & Sun, D. (2010). Improving the representation of thermal boundary conditions of livestock during CFD modelling of the indoor environment. *Computers and Electronics in Agriculture, 73*(1), 17-36.

Norton, T., Kettlewell, P., & Mitchell, M. (2013). A computational analysis of a fully- stocked dual-mode ventilated livestock vehicle during ferry transportation. *Computers and Electronics in Agriculture, 93,* 217-228.

Pawar, S. R., Cimbala, J. M., Wheeler, E. F., & Lindberg, D. V. (2007). Analysis of Poultry House Ventilation Using Computational Fluid Dynamics. *Transactions*

of the ASABE, 50(4), 1373-1382.

Ritz, C. W., Webster, A. B., & Czarick, M. (2005). Evaluation of Hot Weather Thermal Environment and Incidence of Mortality Associated with Broiler Live Haul. *The Journal of Applied Poultry Research, 14*(3), 594-602. doi:10.1093/japr/14.3.594

Rojano, F., Bournet, P., Hassouna, M., Robin, P., Kacira, M., & Choi, C. Y. (2015). Modelling heat and mass transfer of a broiler house using computational fluid dynamics. *Biosystems Engineering, 136*, 25-38. doi:10.1016/j.biosystemseng.2015.05.004

Rong, L., Bjerg, B., & Zhang, G. (2015). Assessment of modeling slatted floor as porous medium for prediction of ammonia emissions – Scaled pig barns. *Computers and Electronics in Agriculture, 117*, 234-244.

Schwartzkopf-Genswein, K., Faucitano, L., Dadgar, S., Shand, P., González, L., & Crowe, T. (2012). Road transport of cattle, swine and poultry in North America and its impact on animal welfare, carcass and meat quality: A review. *Meat Science*, 227-243.

Stikeleather, L. F., Morrow, W. E., Meyer, R. E., Baird, C. L., & Halbert, B. V. (2012). CFD Simulation of Gas Mixing for Evaluation of Design Alternatives for On- Farm Mass Depopulation of Swine in a Disease Emergency. ASABE Annual International Meeting Presentation. Paper Number: 12-1338237, ASABE, St. Joseph, MI

Tao, X., & Xin, H. (2003). Acute Synergistic Effects Of Air Temperature, Humidity, And Velocity On Homeostasis Of Market–Size Broilers. *Transactions of the ASAE, 46*(2), 491-497

Turnpenny, J., Mcarthur, A., Clark, J., & Wathes, C. (2000). Thermal balance of livestock. *Agricultural and Forest Meteorology, 101*(1), 15-27.

Webster, A., Tuddenham, A., Saville, C., & Scott, G. (1993). Thermal stress on chickens in transit. *British Poultry Science*, 267-277.

Wu, W., Zhai, J., Zhang, G., & Nielsen, P. V. (2012). Evaluation of methods for determining air exchange rate in a naturally ventilated dairy cattle building with large openings using computational fluid dynamics (CFD). *Atmospheric Environment, 63*, 179-188.